Estimating irrigation water use from remotely sensed evapotranspiration data: Accuracy and uncertainties across spatial scales

Authors: Sam Zipper[1,2,*], Jude Kastens[3], Timothy Foster[4], Brownie Wilson[1], Forrest Melton[5], Ashley Grinstead[1,6], Jillian M. Deines[7], James J. Butler[1], Landon T. Marston[8]

Affiliations:

1. Kansas Geological Survey, University of Kansas, Lawrence KS 66047
2. Department of Geology, University of Kansas, Lawrence KS 66045
3. Kansas Biological Survey & Center for Ecological Research, University of Kansas, Lawrence KS 66047
4. School of Engineering, University of Manchester, Manchester, UK
5. Atmospheric Science Branch, Earth Science Division, NASA Ames Research Center, Moffett Field, CA 94035
6. Department of Natural Resources and the Environment, University of Connecticut, Storrs, CT 06269, United States
7. Earth Systems Predictability and Resiliency Group, Pacific Northwest National Laboratory, Richland, WA 99354
8. Department of Civil and Environmental Engineering, Virginia Tech, Blacksburg VA 24061

*Correspondence to samzipper@ku.edu

Highlights [3-5, max 85 characters]:

- Compared ET-based irrigation volumes to reported water use data at multiple scales
- ET-based irrigation volumes and reports agreed best when averaged over multiple years
- Soil moisture storage change can bias ET-based irrigation volumes in individual years
- Variation among ET models is substantial relative to irrigation management actions
- ET-based irrigation tracking is promising but application-relevant uncertainties exist

This is a draft manuscript submitted to Agricultural Water Management for peer review (February 28, 2024).

Abstract: Irrigated agriculture is the dominant use of water globally, but most water withdrawals are not monitored or reported. As a result, it is largely unknown when, where, and how much water is used for irrigation. Here, we evaluated the ability of remotely sensed evapotranspiration (ET) data, integrated with other datasets, to calculate irrigation water withdrawals and applications in an intensively-irrigated portion of the central United States. We compared irrigation calculations based on OpenET data with reported groundwater withdrawals from a flowmeter database and hundreds of farmer irrigation application records at three spatial scales (management area, water right group, and field). We found that ET-based calculations of irrigation exhibited similar temporal patterns as flowmeter data, but tended to be positively biased with substantially more interannual variability than reported pumping rate. Disagreement between ET-based irrigation calculations and reported irrigation was strongly correlated with annual precipitation. Agreement between calculated and observed ET was better for multi-year averages than for individual years across all spatial scales. The selection of an ET model was also an important consideration, as variability in calculated irrigation across an ensemble of satellite-driven ET models was larger than the potential impacts of conservation measures employed in the region. Linking individual wells to specific fields was challenging, but uncertainties in calculating irrigation depths due to the above-mentioned factors exceeded potential uncertainty from irrigation status and field boundary mapping. From these results, we suggest key practices for working with ET-based irrigation data that include accurately accounting for changes in root zone soil moisture for within-season applications, such as irrigation scheduling, and conducting an application-specific evaluation of sources of uncertainty. Remotely-sensed approaches have a high potential for improving scientific research and water resource management through improved spatial and temporal characterization of irrigation, but uncertainties must be resolved to fully realize this potential.

Keywords: OpenET, remote sensing, evapotranspiration, water management, High Plains Aquifer, uncertainty

Graphical Abstract:

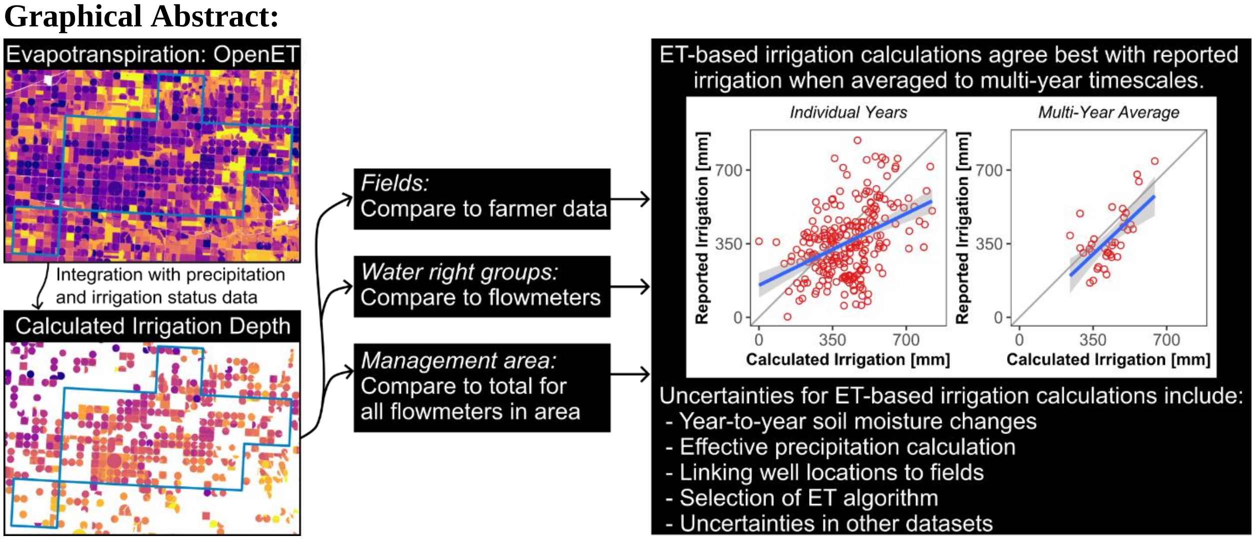

1. Introduction

Irrigated agriculture is the dominant global user of water. Groundwater supplies an estimated 40% of global irrigation, with this figure rising even higher in semi-arid/arid regions or in drought years when surface water availability is limited (Gleeson et al., 2020). As such, groundwater use plays a critical role in global food production and trade (Dalin et al., 2017) and sustaining local and regional economies (Deines et al., 2020). However, groundwater use can also lead to detrimental outcomes, such as the depletion of interconnected surface water resources (de Graaf et al., 2019; Zipper et al., 2022), declining water levels and storage capacity in regionally- and globally-important aquifers (Hasan et al., 2023; Jasechko et al., 2024), and associated water scarcity and insecurity (D'Odorico et al., 2019; Marston et al., 2020). In many agricultural settings without alternative water sources, pumping reductions are the only currently viable tool available to reduce water abstraction and slow water table decline rates (Butler et al., 2020).

Making informed management decisions requires information about pumping rates and the anticipated impacts on the environment (Foster et al., 2020). However, management is challenging because data on the locations, schedules, and volumes of groundwater withdrawals are rarely available, even in data-rich countries like the United States (Marston, Abdallah, et al., 2022). Given the paucity of groundwater pumping data, emerging application-ready remote sensing products may be a valuable tool to fill this data gap (Melton et al., 2022). While flowmeters on pumping wells directly monitor the amount of water coming out of the ground, which we refer to here as 'irrigation water withdrawals', remotely sensed approaches typically provide data for spatially distributed evapotranspiration (ET) rates. Satellite-based ET data can then be incorporated into a water balance or statistical model to infer 'irrigation water applications', or the amount of water that is applied to a field after accounting for losses (Dhungel et al., 2020; Folhes et al., 2009; Foster et al., 2019). Like all modeled quantities, however, these ET-based calculations of irrigation applications are subject to numerous uncertainties, which can lead to inefficient or inequitable water management decisions if not well-characterized (Foster et al., 2020).

Unfortunately, due to the lack of reliable irrigation water withdrawal and application data for ground-truthing, there have been limited opportunities to evaluate the ability of ET-based approaches to calculate irrigation withdrawals and applications. While many past studies have sought to estimate irrigation water use using satellite-based ET data and other hydrological variables such as soil moisture (Brocca et al., 2018; Dari et al., 2020; Ketchum et al., 2023), these estimates have typically been evaluated against aggregated statistics or synthetic model estimates of water use. Other studies use statistical or machine learning approaches to relate ET to observed water use, but these approaches are limited in terms of their applicability outside of the model training region (Filippelli et al., 2022; Majumdar et al., 2022; Wei et al., 2022). As a result, there is a lack of knowledge about how effectively ET data can be translated into irrigation water withdrawals and applications across different spatial scales, from an individual field to a region, which are relevant to regulatory and management purposes.

Here, we address this gap by comparing calculations of ET-based irrigation application and reported irrigation at multiple spatial scales (management area, water right group, field). Reported irrigation data is from both a high-quality flowmeter database of irrigation water withdrawals and direct farmer-provided records of irrigation water applications (Figure 1). Specifically, we ask:

(1) How well do irrigation calculations derived from remotely sensed data and other spatial datasets agree with water withdrawal and application data from flowmeters and farmer records?

(2) What are the major sources of uncertainty in calculating irrigation withdrawals and applications using remotely-sensed ET data?

Addressing these questions provides insights into the potential for remotely sensed ET products to address critical water management issues and highlights key future research needed to operationalize these tools for irrigation mapping and water conservation assessment.

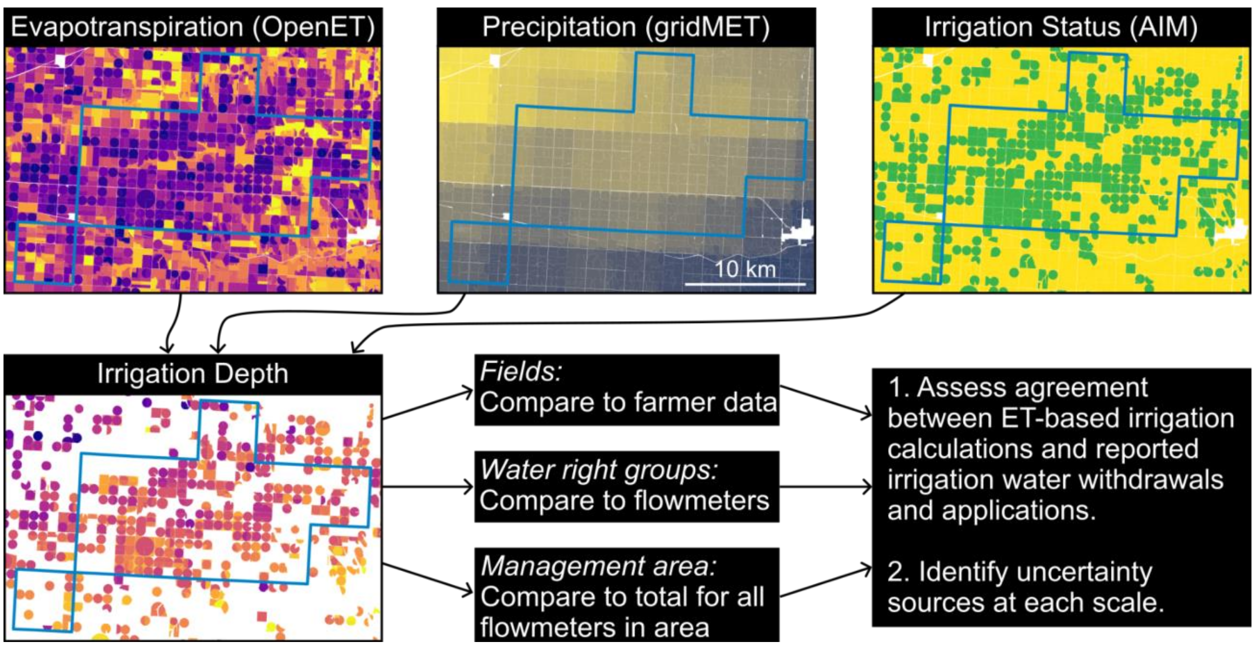

Figure 1. Overview of study including key input datasets (OpenET: Melton et al., 2022; gridMET: Abatzoglou, 2013; AIM: Deines, Kendall, Crowley, et al., 2019), spatial scales, and study objectives. The images show the area in and around the Sheridan-6 Local Enhanced Management Area (blue outline), the location of which is shown in Figure 2.

2. Methods

2.1 Study areas and irrigation ground data

We conducted our comparison of ET-based irrigation calculations to in-situ measurements of groundwater withdrawals and applications at three spatial scales that address different potential use cases for remotely sensed irrigation data:

(1) At the management area scale (Section 2.1.1), we compared ET-based volumes to total irrigation water withdrawals within a 255 km^2 groundwater management area, the Sheridan-6 Local Enhanced Management Area (SD-6 LEMA; blue area in Figure 1 and Figure 2).
(2) At the water right scale (Section 2.1.1), we subdivided the SD-6 LEMA into water right groups (WRGs) made up of non-overlapping combinations of pumping wells, fields, and authorized places of use and compared ET-based irrigation volumes to total water withdrawals within each WRG.
(3) At the field scale (Section 2.1.2), we compared ET-based calculated irrigation depths to field-resolution irrigation water application data from fields where farmers voluntarily shared irrigation records (field-years of data by region shown in Figure 2 in parenthesis).

Conducting our analysis at these three spatial scales allowed us to leverage independent data sources for comparison (a state database at the management area and water right scale, farmer records at the field scale) and address different aspects of uncertainty (i.e., linking locations of water withdrawals to locations of applications was required at the water right scale).

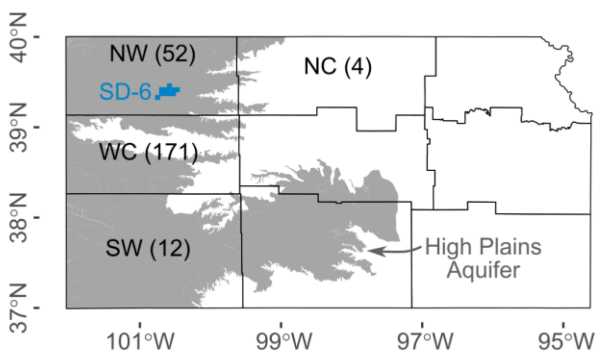

Figure 2. Map of the state of Kansas subdivided into agricultural reporting districts. The location of the Sheridan-6 (SD-6) Local Enhanced Management Area is shown in blue. The number of field-years of data at the field-resolution scale are shown in parentheses for the northwest (NW), north-central (NC), west-central (WC), and southwest (SW) reporting districts within the state. The Kansas portion of the High Plains Aquifer is shown in gray.

2.1.1 Sheridan-6 Local Enhanced Management Area

The Sheridan-6 Local Enhanced Management Area (SD-6 LEMA) covers 255 km^2 in northwest Kansas, much of which is used to grow irrigated corn, soybeans, sorghum, and wheat (Figure 2; Figure S1). The SD-6 LEMA was formed when local irrigators, concerned about declining groundwater levels, proposed an allocation of 1397 mm (55”) of water over a five-year period, which represented an approximate 20% reduction in pumping rates compared to historical averages (Drysdale & Hendricks, 2018). After approval by the state’s chief engineer, this allocation was codified in law for a five year period beginning in 2013. The irrigators within the SD-6 LEMA have since renewed for two additional five year periods (2018-2022 and 2023-2027). To date, the SD-6 LEMA exceeded the original conservation goals and reduced irrigation water withdrawals by 26-31% (Deines, Kendall, Butler, et al., 2019; Drysdale & Hendricks, 2018) and slowed water table decline rates (Butler et al., 2020; Whittemore et al., 2023) with only minor negative impacts on yield and none on profitability (Golden, 2018). As such, the SD-6 LEMA is a successful example of irrigator-driven groundwater conservation (Marston, Zipper, et al., 2022) and has motivated the development of additional conservation approaches around the state (Steiner et al., 2021).

We selected the SD-6 LEMA as the focus of our management area and water right scale comparison because conservation practices have led to high irrigation efficiencies of producers in the SD-6 LEMA with relatively little wasted irrigation water (e.g., deep percolation from return flows or major fluxes of soil evaporation caused by excessive irrigation; Deines et al., 2021). High irrigation efficiency suggests that irrigation water withdrawals and applications should be approximately equal to each other and ET-based approaches may be particularly effective for calculating irrigation volumes in this setting. Additionally, due to numerous past studies of groundwater use in the SD-6 LEMA (Deines et al., 2021; Deines, Kendall, Butler, et al., 2019; Dhungel et al., 2020; Drysdale & Hendricks, 2018; Glose et al., 2022; Whittemore et al., 2023), we have a high degree of confidence in the accuracy of the irrigation withdrawal data for the SD-6 LEMA.

Irrigation withdrawal data were aggregated from the Water Information Management and Analysis System (WIMAS; https://geohydro.kgs.ku.edu/geohydro/wimas/) database maintained by the Kansas Department of Agriculture - Division of Water Resources and the Kansas Geological Survey. Withdrawal data are at the resolution of points of diversion, which in the SD-6 region correspond exclusively to pumping wells since there are no surface water resources used for irrigation. The data are high quality, as all non-domestic pumping wells in the state of Kansas are required to use a totalizing flow meter subject to accuracy checks from the Kansas Department of Agriculture (Butler et al., 2016). We also used reported irrigated acreage from the WIMAS database, though unlike water use, the reported irrigated acreage is not subject to verification and therefore the accuracy is unknown. In the SD-6 LEMA, we conducted our comparison at two spatial scales:

- For the management area scale comparison, we summed the total annual withdrawals from all irrigation wells within the SD-6 LEMA boundaries. For any water rights that had authorized places of use both inside and outside the LEMA (n = 9, or 6% of the total water right groups), we scaled the total water use based on the proportion of total estimated irrigated area that was within the LEMA for that well. This is the approach used in Brookfield et al. (2023) and is extended here through additional analyses of uncertainty, the use of effective precipitation for estimating irrigation depths, and comparison to other spatial scales.
- For the water right group (WRG) scale comparison, we established non-overlapping groups of water withdrawals and applications by combining wells, water rights, and authorized places of use as in Earnhart & Hendricks (2023). This aggregation was necessary due to the complexities of agricultural water management that make it

impossible to quantify the water use for a specific field from the WIMAS data alone: (i) a single well may provide water to multiple fields; (ii) a single field may receive water from multiple wells; (iii) a single water right may cover multiple wells and fields; and (iv) irrigators are only required to report the authorized place of use and the total number of acres irrigated, not the specific locations where water was used within the authorized area in a specific year. For each WRG, we then summed the total reported annual water withdrawals for all wells within the WRG. To evaluate potential errors associated with defining WRGs, we also compared reported irrigated acreage for all the wells in the WRG (from WIMAS) to estimated irrigated acreage based on the fields mapped as irrigated within the authorized place of use for each WRG. Irrigated fields were identified based on previously published remotely-sensed irrigation maps for each year in the Annual Irrigation Maps (AIM) dataset (Deines, Kendall, Crowley, et al., 2019).

The SD-6 LEMA comparisons were conducted for the period 2016-2020, as that is the extent covered by all necessary input datasets (described in Section 2.2).

2.1.2 Individual fields

For an independent additional comparison, we also collected field-resolution irrigation application information from four farmers willing to share this information with us. Farmers were contacted directly based on existing personal relationships and through regional organizations such as groundwater management districts and asked to provide applied irrigation volumes for as many fields as they were willing to share at the finest possible temporal resolution. We also requested either data files or annotated pictures showing the irrigated extent for each field so we could extract satellite-based ET data for each field. Unlike the management area and WRG scale comparisons, therefore, for the field-scale comparison we had reported data specifying actual places of use and irrigated extent. Irrigation data we received included minute-resolution water use from irrigation control software, irregularly timed sub-annual water use based on periodic visits to flowmeters, and annual values based on flowmeter data that farmers associated with specific fields. For this study, all data were aggregated to the annual total depth of applied irrigation. In total, we received data for 43 fields between 2016 and 2022, totaling 239 field-years of data. To protect the privacy of the farmers involved (Zipper, Stack Whitney, et al., 2019), the locations of the fields are only shown here at the resolution of federal agricultural reporting districts (Figure 2). The data span three of the five reporting districts that overlie the High Plains Aquifer, with the most fields in west-central and northwest Kansas (note: one field, just across the border in Nebraska, is included with the NW Kansas district). None of the fields included within this dataset are within the SD-6 LEMA.

2.2 Calculating irrigation from ET data

We integrated ET data with several other geospatial datasets to calculate irrigation volumes and/or depths (Figure 1). We extracted OpenET data from Google Earth Engine at a monthly time step for 2016-2022 (Melton et al., 2022). OpenET includes ET data from six different satellite-driven models, as well as an ensemble mean. The models included are DisALEXI (Anderson et al., 2007, 2018), eeMETRIC (Allen et al., 2005, 2007, 2011), geeSEBAL (Bastiaanssen et al., 1998; Laipelt et al., 2021), PT-JPL (Fisher et al., 2008), SIMS (Melton et al., 2012; Pereira, Paredes, Melton, et al., 2020), and SSEBop (Senay et al., 2022). The ensemble mean was calculated as the mean of all models, with outlier values from the ensemble identified based on median absolute deviations and removed prior to calculation of the ensemble mean (Volk et al., 2024). The OpenET products were validated against 70 eddy covariance towers deployed at agricultural sites spanning a range of climate and land cover conditions across the western US and generally had a strong agreement, with all models within +/- 15% of growing season mean flux tower ET averaged across all sites (Melton et al., 2022). A subsequent evaluation affirmed the accuracy of the ET data from OpenET via comparison to a total of 141 sites with eddy covariance towers, along with seven sites with Bowen ratio systems and four weighing lysimeters, finding that the growing season ensemble ET values for cropland had a mean absolute error of 78.1 mm (13.0%) and a mean bias error of -11.9 mm (2.0%). The overall accuracy for cropland sites was the best of any land cover type evaluated, and performance for annual crops, including corn, soybeans and wheat, was particularly strong (Volk et al., 2024). However, there were no eddy covariance towers near our study area - the closest irrigated fields with eddy covariance towers were in Mead, NE, where annual precipitation is ~50% greater than western Kansas - and therefore OpenET's accuracy for irrigated agriculture in semi-arid conditions typical of the western High Plains Aquifer has not been locally assessed.

OpenET data and precipitation data (from the 4 km gridMET data; Abatzoglou, 2013) were averaged for each field. For the field-resolution comparison, field boundaries, crop type, and irrigation status were defined based on information provided by farmers. For the management area and WRG comparisons, field boundaries were defined based on a Kansas-specific modification of the US Department of Agriculture (USDA) Common Land Unit dataset (Gao et al., 2017; MardanDoost et al., 2019), annual crop type from the USDA Cropland Data Layer (USDA, 2022), and irrigation status from AIM (Deines, Kendall, Crowley, et al., 2019). For crop type and irrigation status, we summarized the rasterized input data to a single categorical value for each field based on the most common raster value. To evaluate potential impacts of this approach, we evaluated confidence in the field-resolution irrigation classifications by evaluating the area of fields with a mixture of irrigated and non-irrigated pixels in the AIM dataset. The irrigation confidence results suggested that this irrigation status mapping approach was more likely to overestimate, rather than underestimate, irrigated area (Figure S3, Figure S4) due to field boundaries not perfectly aligning with on-the-ground management divisions.

To calculate irrigation using our ET data (Figure 1), we calculated the precipitation deficit (ET - effective precipitation) for each field (Figure S5) and masked it to only fields mapped as irrigated (Figure S6). Effective precipitation was calculated as precipitation from gridMET minus deep percolation out of the bottom of the root zone, which we estimated as a function of precipitation based on 2013-2017 deep percolation estimates from Deines et al. (2021) (regressions shown in Figure S9). This method does not account for soil moisture storage from year-to-year, so we carried out these calculations at three timescales: the growing season (April-October), the calendar year (January-December), and the water year (October-September). This allowed us to test the degree to which the timescale of aggregation influenced agreement with reported irrigation withdrawal data. Since negative irrigation depths are not physically possible, for any irrigated fields with a negative precipitation deficit we set the irrigation depth to 0 mm, though this was rare (Figure S5). Irrigation depth was calculated separately for each year and each model (six ET models, as well as the ensemble mean). Since there are no surface water rights in this region, we assumed that all irrigation was sourced from groundwater. Our approach to estimating irrigation adopts several assumptions, including that there is minimal runoff or fluxes of water apart from precipitation, irrigation, deep percolation and evaporation. While past work has suggested that there is virtually no runoff under conservation practices in the SD-6 LEMA (Deines et al., 2021), these assumptions may be less appropriate in other parts of the state, in particular the 4 field-years of data in the north-central region (Figure 2). Additionally, there may be differences in the relationship between precipitation and deep percolation in other regions given that irrigation efficiency is particularly high in the SD-6 LEMA. To assess the potential impacts of our effective precipitation estimates on our findings, we repeated all analyses using actual precipitation (instead of effective precipitation) in our precipitation deficit calculations, and these results are shown in the Supplemental Information Section SI3.

3. Results

3.1 Management area comparison

At the scale of the SD-6 LEMA, the ET-based irrigation volumes are the same order of magnitude as the reported withdrawal values but have a positive bias and greater interannual variability (Figure 3, Table 1). Agreement between estimated irrigation and reported water withdrawals is fairly similar regardless of whether irrigation is estimated based on the calendar year, growing season, or water year. The best-performing model and timescale depend on the fit metric being used (Table 1). For instance, the average mean absolute error (MAE) value across all models was lowest for the water year-based irrigation volumes, but the growing season irrigation volumes based on geeSEBAL had the lowest MAE of any model or timescale. Broadly, we interpret the performance of satellite-based irrigation water withdrawals to be best when the growing season is used as the temporal unit of aggregation as, averaged across all models, this timescale has close to the lowest MAE, the slope closest to 1.0, and intermediate bias and R^2 compared to other timescales.

The relatively high R^2 values we observe across all both the calendar year and growing season timescales of aggregation (generally $R^2 > 0.9$), combined with the relatively high MAEs (~1-2 x10^7 m^3, which is approximately equal to typical irrigation withdrawals for the management area) and a slope lower than one (Table 1) collectively support our interpretation that the ET-based irrigation calculations capture appropriate temporal patterns of variability in estimated irrigation, but tend to overestimate both the average magnitude and degree of interannual variability in irrigation volumes. As a result, when averaged across the full time period (2016-2020) the ET-based approaches tend to fall above the range of reported variability, with the lowest bias from geeSEBAL and the highest bias from SIMS. The high calculated irrigation volumes from SIMS make sense due to the formulation of this model, which assumes well-watered conditions sufficient to meet the needs of the satellite-observed crop density (Melton et al., 2012). Even irrigated crops in this region likely experience periodic water stress during the growing season, as evidenced by the narrow distribution of SIMS ET data with respect to other models (Figure S7). Since the overestimates we observed suggest that our estimated effective precipitation values may be too low, we repeated our analyses using actual precipitation in our irrigation calculations (Section SI3). In this case, we found that the ET-based irrigation calculations better captured the central tendency of the reported data but have greater year-to-year variability characterized by underestimates in wet years and overestimates in dry years (Figure S10a-c, Figure S12). As a result, the agreement between the reported and calculated irrigation volumes based on actual precipitation was substantially better when averaged across multiple years because this averaged out opposing positive and negative errors in dry and wet years, respectively (Figure S10d-f).

At the annual resolution, the differences between the ET-based irrigation volumes and the reported groundwater withdrawals are strongly responsive to growing season weather conditions, whether irrigation was calculated using effective precipitation (Figure 4a) or actual precipitation (Figure S12). The ET-based approaches overestimated the metered irrigation volumes the most in dry years, such as 2020, and the least in wet years, such as 2019 (Figure 4a). Based on this, we tested whether precipitation could be used to statistically adjust ET-based irrigation calculations to better match reported irrigation volumes (Figure 4b). For each ET model, we developed a linear regression between the irrigation volume residual (shown for the ensemble mean in Figure 4a) and used this linear relationship to adjust ET-based irrigation calculations. The resulting precipitation-adjusted irrigation calculations, shown in Figure 4b, had a substantially better agreement with reported irrigation values, with reductions in MAE by one to two orders of magnitude, and four of the models and the ensemble mean had slopes between 0.9 and 1.1 after adjustment (full fit statistics in Table S1). Relationships were similarly strong when using actual, instead of effective, precipitation for irrigation calculations (Figure S12).

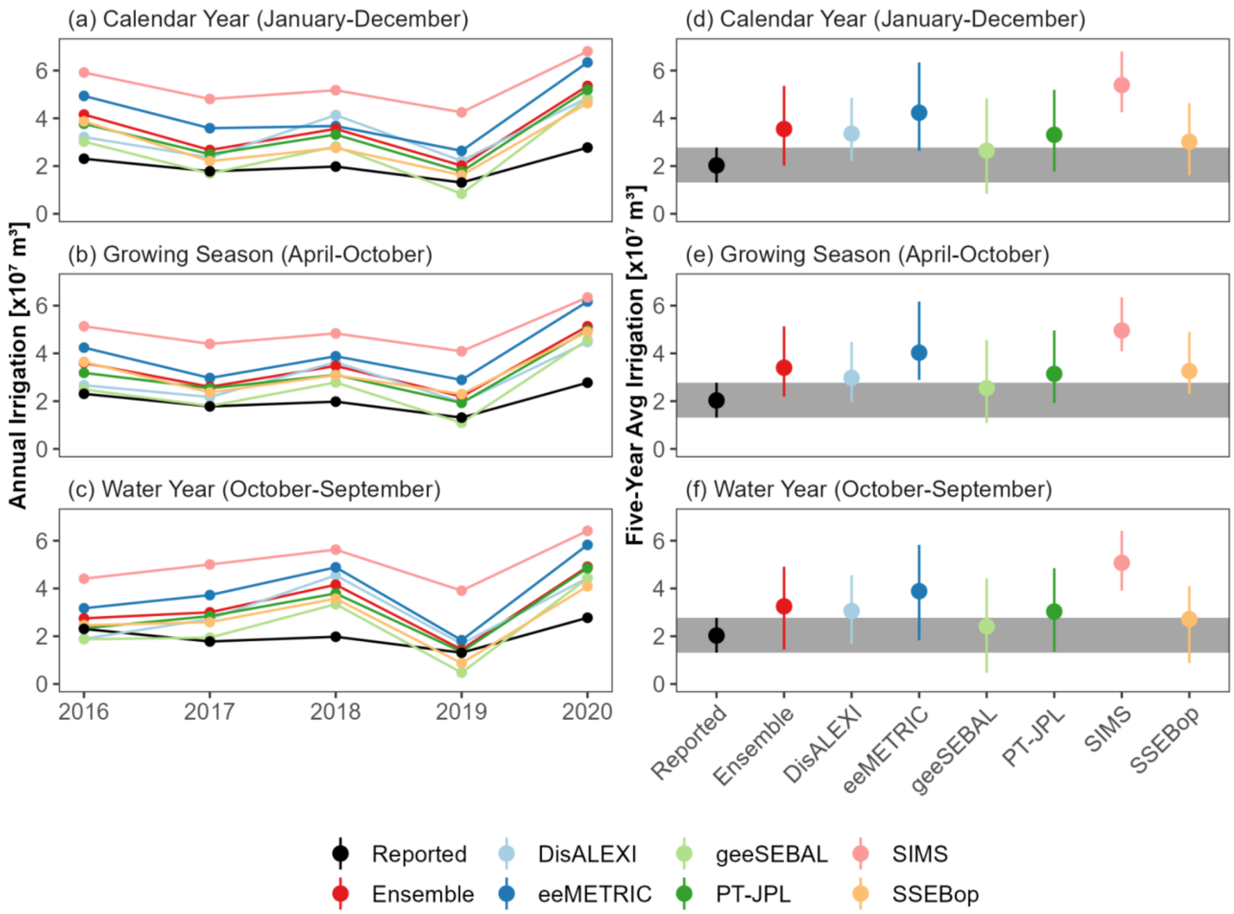

Figure 3. Comparison between reported WIMAS pumping and ET-based irrigation volumes from (a, d) annual, (b, e) growing season, and (c, f) water year precipitation deficit over the entire SD-6 LEMA. The left column (a-c) shows a comparison at annual resolution, and the right column (d-f) shows the five-year average as a point with the five-year range as error bars. The gray shading in the background shows the range of the reported values over the period.

Table 1. Fit statistics for annual-resolution LEMA-scale OpenET-WIMAS comparison for each timescale of aggregation and model. 'C.Y.' = Calendar Year, 'G.S.' = Growing Season, 'W.Y.' = Water Year. Yellow shading indicates model with the best performance for that statistic and timescale. Blue shading indicates best performance for that fit metric across all timescales. The red shading in the 'Average' row indicates the best performing timescale across all models. Results shown in bar-chart form in Figure S8.

	MAE [x10^7 m^3]			**Bias [%]**			**Slope**			**R^2**		
Model	*C.Y.*	*G.S.*	*W.Y.*	*C.Y.*	*G.S.*	*W.Y.*	*C.Y.*	*G.S.*	*W.Y.*	*C.Y.*	*G.S.*	*W.Y.*
DisALEXI	1.33	0.95	1.19	65%	47%	51%	0.41	0.43	0.23	0.71	0.69	0.32
eeMETRIC	2.20	2.00	1.86	109%	99%	92%	0.38	0.39	0.29	0.97	0.88	0.64
Ensemble	1.52	1.37	1.22	75%	68%	60%	0.42	0.47	0.34	0.98	0.93	0.67
geeSEBAL	0.84	0.60	0.89	30%	25%	19%	0.36	0.40	0.31	0.96	0.89	0.71
PT-JPL	1.28	1.11	1.00	63%	55%	49%	0.42	0.46	0.33	0.98	0.92	0.64
SIMS	3.36	2.93	3.04	166%	144%	150%	0.55	0.61	0.42	0.98	0.93	0.57
SSEBop	0.99	1.23	0.86	49%	61%	34%	0.44	0.49	0.37	0.97	0.91	0.69
Average	1.65	1.46	1.44	79%	71%	65%	0.42	0.46	0.32	0.94	0.88	0.61

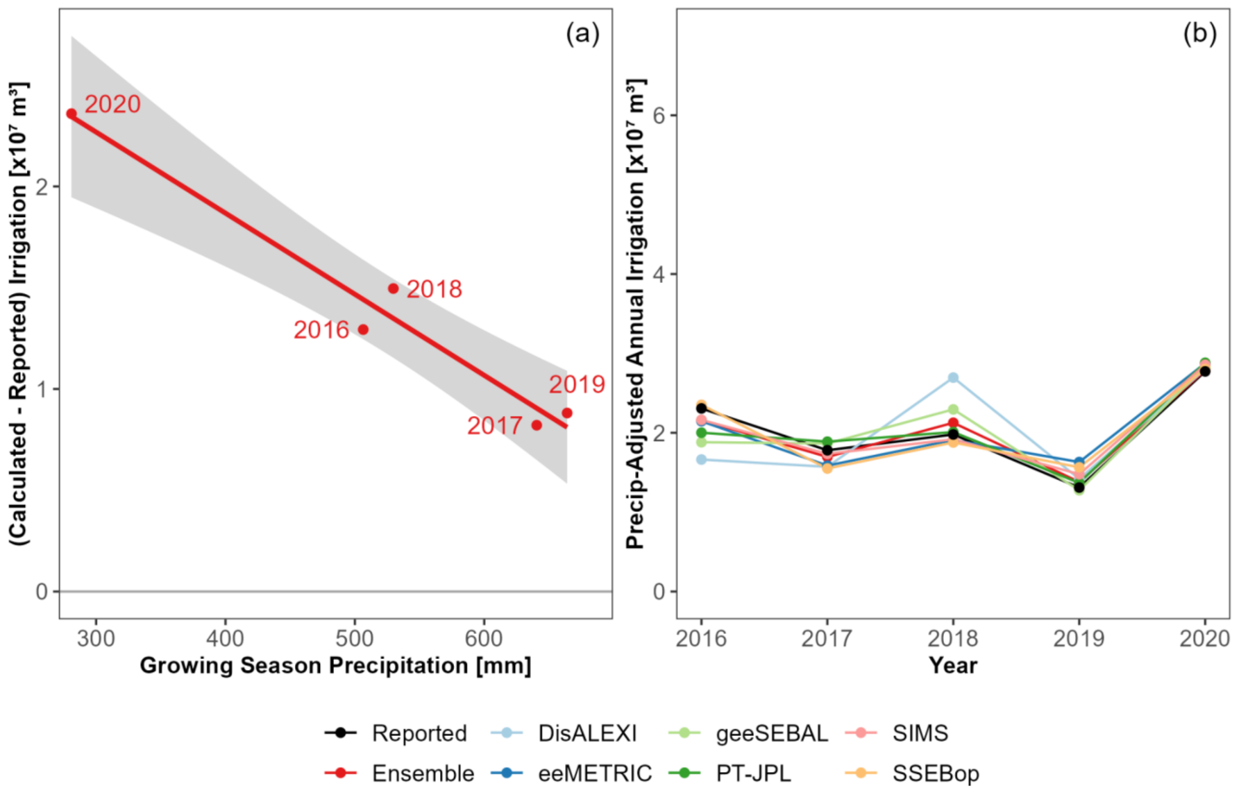

Figure 4. Impacts of precipitation on ET-based irrigation calculations. (a) Difference between ET-based calculated irrigation volume (from the OpenET ensemble) and reported water withdrawals for the SD-6 LEMA as a function of total growing season precipitation. A positive value means that the ET-based irrigation volume was higher than the reported total. The red line indicates a linear best-fit with a shaded standard error confidence interval ($R^2 = 0.96$) and points are labeled by year. (b) Precipitation-adjusted irrigation volumes for each model compared to reported irrigation volumes. In this plot, each ET-based irrigation calculation was statistically adjusted as a function of precipitation, for example as shown in Figure 4a for the Ensemble. Axis limits in Figure 4b are the same as Figure 3e for comparison.

3.2 SD-6 LEMA water right group comparison

The WRG comparison, like the SD-6 LEMA total comparison, revealed that there was a positive correlation between calculated and reported irrigation, but a general positive bias of calculated irrigation and improved agreement when averaged over multiple years. For the WRG-scale comparison, the growing season-based irrigation volumes from the ensemble ET were used. As with the management area comparison, the estimated irrigation volumes showed substantially more interannual variability than reported irrigation volumes at the WRG scale, with ET-based irrigation volumes higher than reported volumes for most WRGs and years, and the greatest positive bias during dry years such as 2020 (Figure 5a). When averaged across all five years, the scatter in the agreement between estimated and reported irrigation volumes was dramatically reduced (Figure 5c), though the calculated irrigation volumes tended to be positively biased related to reported irrigation as in the management area analysis (Figure 3).

The correlation between estimated and reported irrigation was worse for irrigation depths (Figure 5b, Figure 5d) than volumes (Figure 5a, Figure 5c), though irrigation volumes were more consistently positively biased than depths. Overall, our results indicate that uncertainty in estimated irrigation depth is greater than uncertainty in estimated irrigated area, which is further supported by the field-scale comparison in Section 3.3 and has been observed in other ET-based irrigation comparisons in Nevada and Oregon (Ott et al., 2024). Nevertheless, place of use and irrigation status are potential drivers of some disagreement between calculated and reported irrigation volumes. The irrigated area within WRGs based on annual irrigation maps (Deines, Kendall, Crowley, et al., 2019) very rarely closely matched the reported irrigated area in the WIMAS database. While there was a positive correlation between reported and estimated irrigated area, differences between these two numbers exceeded 10% in 634 of 685 WRG-years, and estimated irrigated area was often higher than reported irrigated area (Figure 6). On average, the estimated irrigated area was 36% higher than the reported irrigated area (median = 28.4%). This indicates that overestimated irrigated area may contribute to overestimated irrigation volumes at both the management area scale and the WRG scale

While irrigated area is required for annual water use reports, water use reports do not include spatial information specifying where the water was actually used, and total irrigated area is not subject to verification or enforcement penalties (unlike reported water use). Therefore, it is unknown how accurate the reported data are, but one plausible explanation for the disagreement in estimated and reported irrigated area is uncertainty in field or parcel boundaries, particularly related to corners of parcels that are irrigated with center-pivot systems. Since the field boundary dataset we are using was originally based on 2007 common land units (CLUs) mapped by the USDA with some refinements (Gao et al., 2017), it may not accurately delineate fields that harbor differently managed component areas. For example, a square quarter section containing a center pivot might consist of separate CLUs for the irrigated circle and the non-irrigated corners, or it might simply be the quarter section boundary with multiple records for differently managed subfields used when the farmer signs up for federal government programs such as crop insurance. In the latter case, the entire field would be classified as irrigated based on our assignment of irrigation by majority, even though the ~20% of the field in the corners would not be reported as irrigated by the farmer. This is consistent with our observation that there tended to be more low-confidence classifications for irrigated fields than non-irrigated fields (Figure S3). Areas of low-confidence classifications were often field corners (Figure S4), suggesting that the misclassification of non-irrigated corners as irrigated due to insufficiently refined field boundaries may inflate our irrigated area estimates.

To assess the potential impacts of errors in irrigated area classification, we repeated the analysis using only WRGs where the reported and estimated irrigated area agreed within 10% (Figure S23). The results of this comparison had a smaller positive bias for both irrigation volumes and depths, with overall the best agreement observed for multi-year average volumes (Figure S23c). While the annual-resolution irrigation depths had a similar overall correlation (Figure 5b and Figure S23b), the correlation between five-year average calculated and reported irrigation depth improved when only using WRGs with strong irrigated area agreement (R^2 = 0.25, Figure S23d) compared to using all WRGs within the LEMA (R^2 = 0.01, Figure 5d).

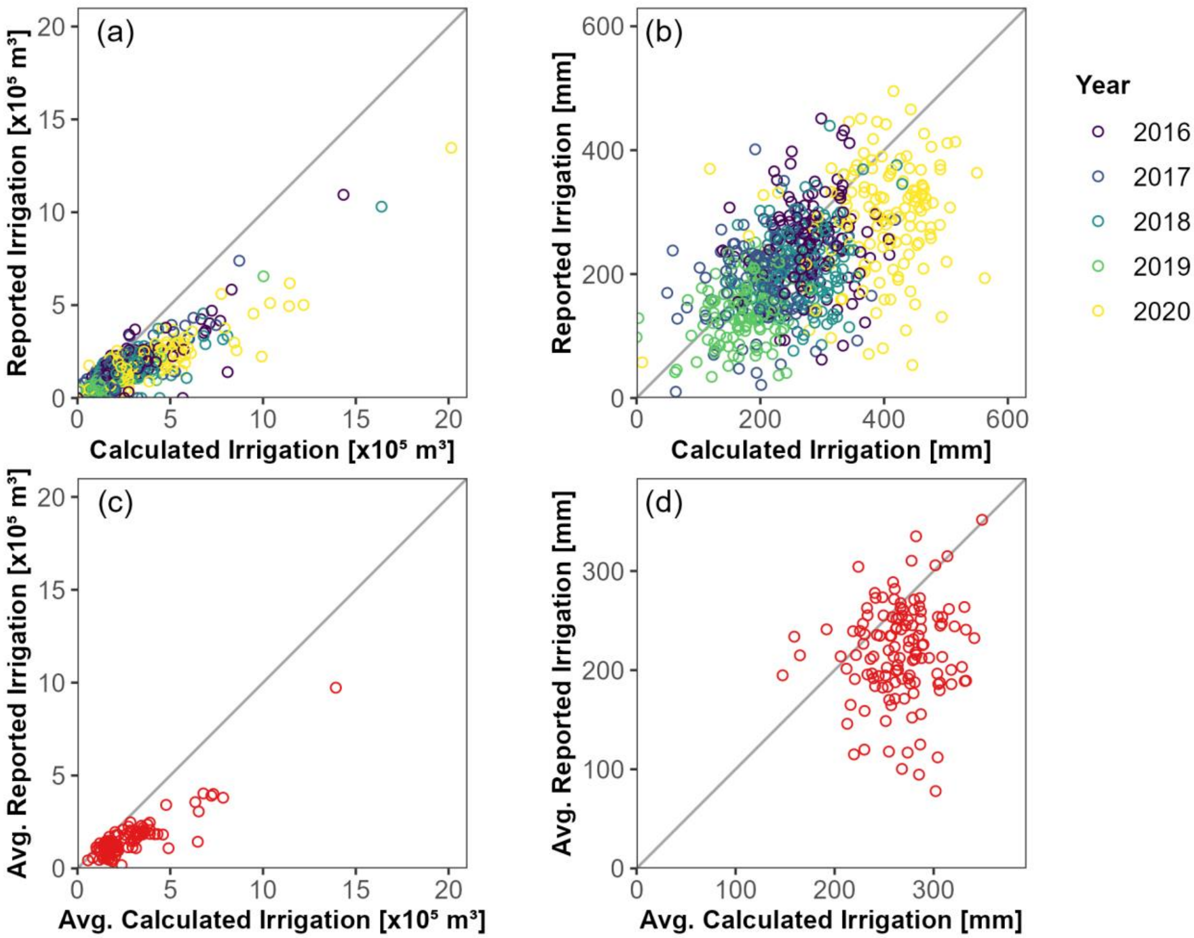

Figure 5. Comparison of reported irrigation for each water right group (WRG) to ET-based irrigation calculation using the ensemble ET. (a) Annual irrigation volume for each WRG; (b) Annual irrigation depth for each WRG; (c) Average irrigation volume for each WRG; (d) Average irrigation depth for each WRG. In each plot, the gray line shows a 1:1 agreement between reported and estimated irrigation.

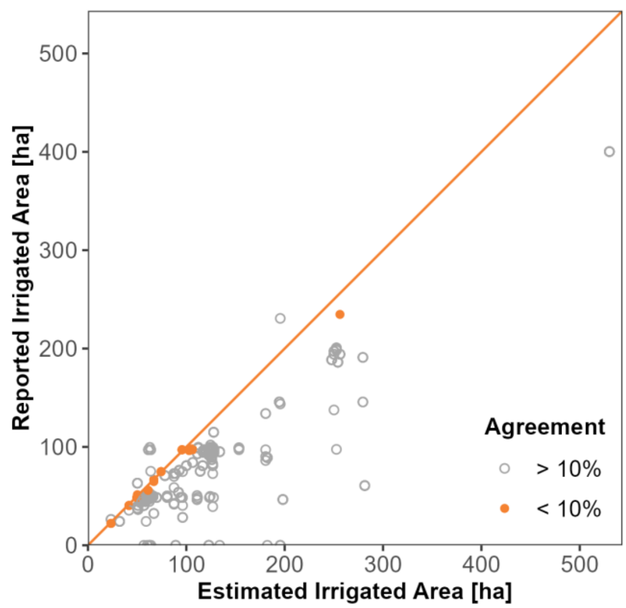

Figure 6. Comparison between reported irrigated area (from WIMAS) and estimated irrigated area (from AIM and authorized places of use) within each water right group in the SD-6 LEMA. Points colored orange have an agreement within 10% and the orange line shows 1:1 agreement.

3.3 Field-scale comparison

At the field scale, we again observed better agreement between calculated and reported irrigation when averaging across multiple years than when looking at individual years (Figure 7, Table 2). At the annual resolution, there was not a strong correlation between calculated and reported irrigation (average R^2 across models = 0.16; Table 2). However, the range of calculated irrigation depths matched the reported depths fairly well, unlike the management area and WRG scales where we observed more consistent overestimates by the ET-based approaches, especially during dry years (Figure 4, Figure 5). Since the fields included here were not part of the SD-6 LEMA, this may reflect lower irrigation efficiencies and increased non-evaporative losses (such as deep percolation or runoff), particularly since our effective precipitation relationship was based on the data from the SD-6 LEMA (Figure S9). Agreement for individual years did not appear to vary systematically as a function of the region within the state, though the dataset was not evenly distributed among regions with the large majority of the fields in either west-central or north-west Kansas (71.5% and 21.8% of total field-years, respectively; Figure 2) which are climatically very similar.

The choice of model also contributed to variability for both individual years and multi-year averages. As we observed for the management area comparison, at the field scale we found a consistent rank ordering, with the lowest calculated irrigation depths by geeSEBAL and the highest by SIMS at both the scale of individual years and multi-year average (Figure 7). When averaged across multiple years, the error in each model was substantially reduced (Table 2). For the multi-year average, we observed the best overall performance by SSEBop, which had the lowest MAE (90 mm), smaller bias than most other models (16.7%), a slope close to one (1.06), and the highest R^2 (0.56) of all models. The DisALEXI and Ensemble irrigation depth calculations also agreed more closely with the reported data than other models, with comparable MAE (99 and 100 mm, respectively) and a slope relatively close to one for the multi-year average.

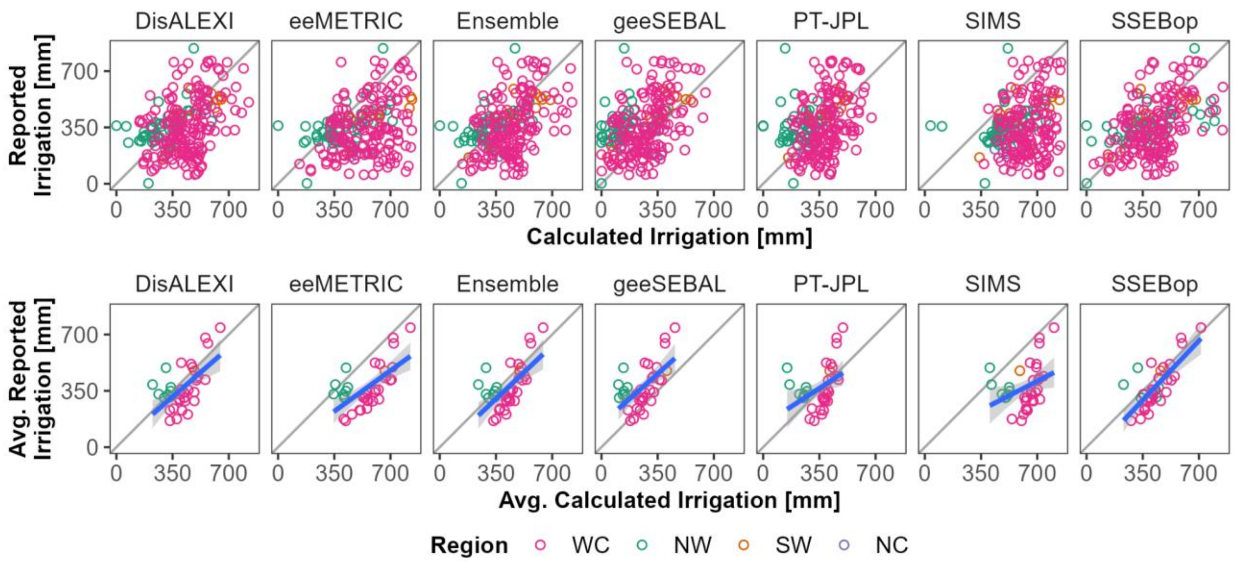

Figure 7. Comparison between reported and calculated irrigation for individual fields. The top row shows annual reported irrigation and the bottom row shows the multi-year average, both colored by the region within the state. In each panel, the gray line indicates 1:1 agreement and the blue lines in the bottom panels show a linear best-fit with a shaded standard error confidence interval.

Table 2. Fit statistics for field-resolution comparison between calculated and reported irrigation application depths.

	MAE [mm]		**Bias [%]**		**Slope**		**R^2**	
Model	*Annual*	*Multi-Year*	*Annual*	*Multi-Year*	*Annual*	*Multi-Year*	*Annual*	*Multi-Year*
DisALEXI	146	99	14.7	12.2	0.47	0.87	0.17	0.36
eeMETRIC	223	190	53.0	49.6	0.33	0.72	0.16	0.42
Ensemble	143	100	16.9	14.4	0.52	0.95	0.20	0.40
geeSEBAL	157	124	-29.5	-31.3	0.54	0.89	0.21	0.37
PT-JPL	140	102	-0.9	-3.3	0.47	0.65	0.11	0.17
SIMS	280	259	72.4	68.2	0.28	0.51	0.06	0.13
SSEBop	144	90	16.7	14.4	0.49	1.06	0.24	0.56
Average	*176*	*138*	*20.5*	*17.7*	*0.44*	*0.81*	*0.16*	*0.34*

4. Discussion

We found that there was generally a positive correlation between calculated and reported irrigation at the management area, WRG, and field scales. However, there was substantially more variability in the ET-based irrigation calculations than reported irrigation, with calculated irrigation often higher than reported irrigation, particularly in dry years. As a result, agreement between reported and calculated irrigation tended to improve when averaged across multiple years. Here, we discuss key sources of uncertainty that may have contributed to differences between reported and calculated irrigation and how those may affect the utility of ET-based irrigation products for research and management.

4.1 Sources of uncertainty in estimating irrigation from ET data

We identified and evaluated several sources of uncertainty that may explain differences between satellite ET-based and reported irrigation water withdrawals and applications, including (i) accounting for non-evaporative water balance components such as changes in soil moisture storage; (ii) variability among models; (iii) linking fields to wells; and (iv) uncertainty in the input datasets that are integrated with ET data to calculate irrigation.

Year-to-year changes in soil moisture appeared to be a primary driver of disagreements between the estimated and reported irrigation at all three spatial scales. Since our approach relies on a relatively simple water balance (ET - effective precipitation) to estimate applied irrigation, this suggests that irrigation is being overestimated by the ET-based approaches in dry years such as 2020 because soil moisture storage in the root zone is being drawn down (Figure 4a). Holding all other aspects of the water balance constant, if soil moisture storage decreased during the dry 2020 growing season, this would cause an overestimate of irrigation since some of the ET in 2020 was using soil moisture that fell in previous years, such as the relatively wet 2019. One contributing factor to our observed overestimates of irrigation may be the relatively simple approach we used to estimate effective precipitation, which was based on a regional regression for deep percolation (Figure SI9), and assumes there is no runoff in the region based on past work (Deines et al., 2021). Since repeating our analysis using irrigation calculated from precipitation (shown in Section SI3) generally showed less bias but greater interannual variability than the effective precipitation approach we used, it suggests that our effective precipitation calculation may be overestimating deep percolation losses, and as a result underestimating the total volume of irrigation applied. The consistent positive precipitation deficit for rainfed corn (Figure 8) further suggests that effective precipitation is being underestimated by our approach, and calculating effective precipitation using a field-specific soil water balance model approach such as ETDemands (Allen et al., 2020) could help to improve overall agreement.

Variability in individual producer irrigation behavior across years may also contribute to the increased interannual variability in the ET-based irrigation volumes observed in Figure 3 compared to the reported irrigation volumes. For example, previous research in the neighboring state of Nebraska has shown that metered groundwater use typically exceeds crop water requirements in wetter or average rainfall years while farmers are observed to adopt more water-efficient irrigation practices in drier years to reduce non-consumptive water losses, likely motivated by a combination of the higher costs of irrigation and greater likelihood of experiencing irrigation system capacity constraints in drought years (Foster et al., 2019). ET-based approaches to calculating irrigation are also unable to capture other water fluxes such as surface runoff. While runoff may be a source of error in our simple water balance approach for some locations (e.g. fields with larger slopes), it is regionally a small component of the water balance and is unlikely to explain systematic patterns of model errors observed across our study area (Deines et al., 2021). Furthermore, our ET-based irrigation volumes did not account for leakage in irrigation systems and other losses of water between where it is pumped from the ground but before it reaches the field, though based on the high efficiency in the SD-6 LEMA area we expect that these losses are minimal. These findings suggest that, for annual or finer temporal resolutions, the use of more complex water balance approaches, such as soil water balance models (Dhungel et al., 2020; Kharrou et al., 2021; Pereira, Paredes, & Jovanovic, 2020), will be necessary to accurately disentangle the rates, locations, and timing of irrigation applications, and there may be promise through the assimilation of additional data sets such as in situ or remotely sensed soil moisture (Dari et al., 2020; Filippelli et al., 2022; Jalilvand et al., 2019).

The selection of ET model also led to substantial variability in the estimated irrigation depths, with a relatively consistent ordering across models (from lowest to highest): geeSEBAL, DisALEXI, PT-JPL, SSEBop, Ensemble, eeMETRIC, SIMS (Figure 3, Figure 7). Since the effective precipitation input data used to estimate irrigation was the same for all models, this variability in estimated irrigation among the models can be attributed to entirely differences in the approaches used by each ET model, and variability can be quite substantial. For example, for irrigated corn in the SD-6 LEMA, the medians span ~156-270 mm across ET models in a given year (Figure 9), which approaches the magnitude of total applied irrigation water and greatly exceeds the magnitude of the conservation actions put in place in this region (Whittemore et al., 2023). The variability among models may be due to differences in the approaches to computation of the sensible heat flux used in each of the five energy balance models, differences in the spatial scale of key meteorological inputs for the DisALEXI, PT-JPL and geeSEBAL models, and model assumptions, especially for SIMS, which assumes well-watered conditions. This underscores the importance of local model accuracy assessments to identify the models that perform best for the crop types and irrigation management practices that are most prevalent in the region. In the absence of suitable independent dataset for use in a local or regional accuracy assessment, OpenET recommends use of the ensemble ET value, which has been shown to perform best overall for the western U.S. across most accuracy metrics (Melton et al., 2022; Volk et al., 2024). We found that the model ensemble was generally among the best-performing approaches to estimating irrigation (as observed in Volk et al., 2024 through comparison with eddy covariance data), particularly after statistically adjusting to account for potential errors in effective precipitation calculations (Figure 4b), suggesting that the ensemble would be a reasonable approach to use across our study region until additional local accuracy assessments can be conducted.

Accurately linking the point of water diversion with the place where that water is applied was a major challenge in our analysis and has been identified as a key source of uncertainty in other domains (Ott et al., 2024). While developing these links may not be needed for many applications, such as estimating regional water use (Figure 3) or field-based water management (Figure 7), connecting the point of diversion with place of use is critical to evaluate irrigation application depths and to assess the effectiveness of conservation measures and the ultimate impacts of pumping on other aspects of regional agrohydrological systems such as streamflow (Kniffin et al., 2020; Zipper, Carah, et al., 2019; Zipper et al., 2021), aquifer dynamics (Feinstein et al., 2016; Peterson & Fulton, 2019; Wilson et al., 2021), or groundwater-dependent ecosystems (Tolley et al., 2019). At the WRG scale, our ET-based calculations of irrigation volume had better agreement than calculations of irrigation depth (Figure 5), consistent with results from the nearby Colorado portion of the Republican River Basin (Filippelli et al., 2022). The weaker relationship between calculated and reported irrigation depth, compared to irrigation volume, reflects the importance of irrigated area as a determinant of overall irrigation volumes (Lamb et al., 2021; Wei et al., 2022). Because irrigated area (which, despite challenges noted elsewhere in the manuscript, e.g. Figure 6, is relatively easier to estimate than irrigation depth) had a strong correlation between estimated and reported data, dividing out this term to convert from irrigation volume to irrigation depth reduced the overall correlation between calculated and reported irrigation applications. Despite exceptionally high-quality water use data for the state of Kansas, the limited linkages between the point of diversion and actual place of use highlights a key data gap for the application of remotely sensed irrigation data for hydrogeological research and management, and a necessary improvement for field-level operationalization.

Estimating irrigation from satellite-based ET requires a variety of datasets in addition to ET, such as irrigation status and precipitation (Figure 1), and each input dataset is subject to its own uncertainties. For ET, we would expect errors in calculated irrigation to increase for periods or regions with increased cloud cover that affect the optical and thermal bands of satellites used by ET models. Since cloud cover is associated with precipitation events, this may have an outsized effect on estimating ET during times when soil moisture is being replenished. The gridded meteorological datasets we use here are also unable to capture the fine-scale variation in precipitation dynamics that can occur during typical convective summer storms in semi-arid regions (Gibson et al., 2017; Mourtzinis et al., 2017), which would have a stronger influence on the field-scale comparisons included in this analysis. To assess this potential uncertainty, we replicated our management area-scale analysis using National Weather Service Advanced Hydrologic Prediction Service radar precipitation data, which is thought to better capture spatial patterns in precipitation in western Kansas (Whittemore et al., 2023), instead of gridMET precipitation. However, the results of the gridMET-based analysis and radar precipitation analysis were very similar to approaches using gridMET precipitation (see Supplemental Information, Section SI4 compared to Section SI3), indicating that precipitation uncertainty was not likely a major driver of differences between reported and calculated irrigation. Additionally, irrigation mapping can be particularly challenging during wet years where the differences in canopy cover and greenness between irrigated and non-irrigated fields are smaller (Xu et al., 2019). While the irrigation extent dataset we used is the best-available for this region and consistently shows differences in precipitation deficit between irrigated and rainfed corn, there is also substantial overlap between their distributions, suggesting that some degree of misclassification is practically assured (Figure 8). This may be particularly challenging in relatively small unirrigated portions of otherwise irrigated fields, such as the non-irrigated corners of center-pivot systems (Figure S4).

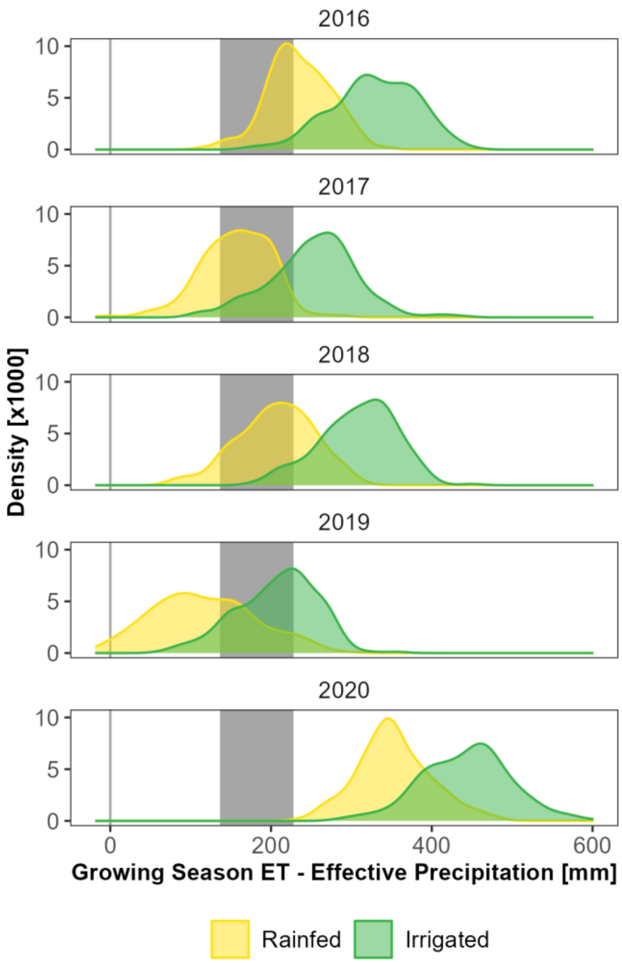

Figure 8. Distribution of field-resolution growing season ensemble ET - Effective Precipitation for corn fields in the LEMA, separated by year and colored by irrigation status. The gray shaded interval shows the average annual reported irrigation depth (182 mm) +/- one standard deviation (46 mm) over the 2016-2020 period.

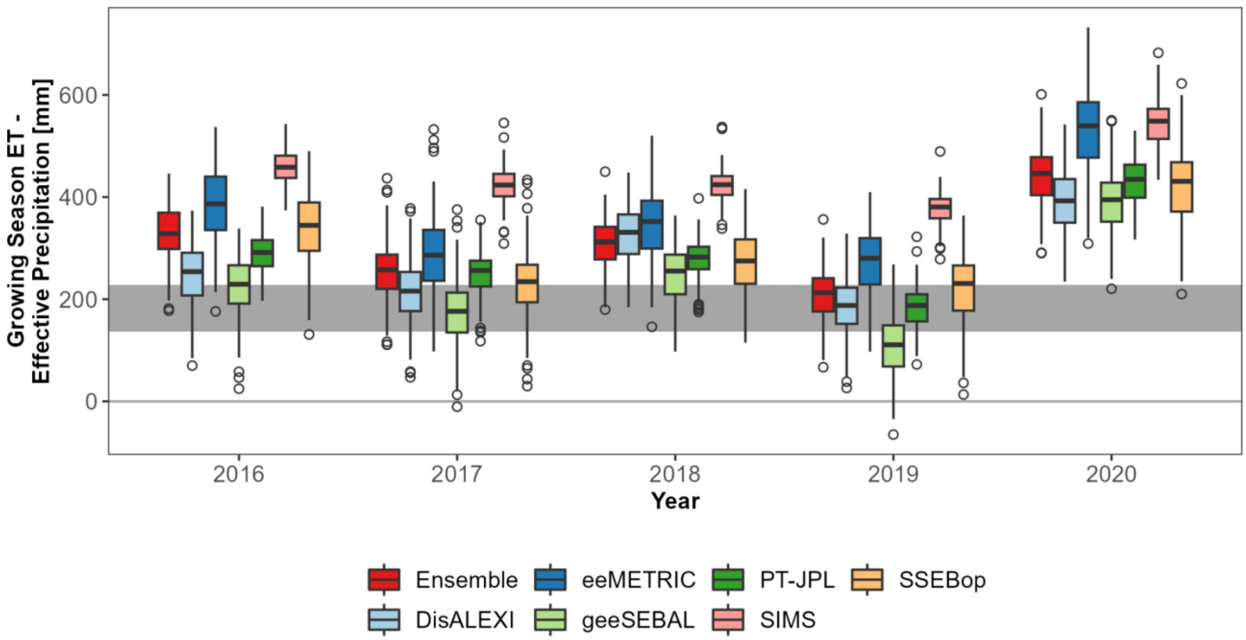

Figure 9. Distribution of ET - precipitation for all irrigated corn fields in the LEMA, colored by model. The gray shaded interval shows the average annual reported irrigation depth (182 mm) +/- one standard deviation (46 mm) over the 2016-2020 period.

4.2 Utility for research and management purposes

As water becomes increasingly scarce, the importance of accurate accounting of how, where, when, and how much water is being used is becoming more critical. In the US, each state is responsible for administering water rights and regulating water use within their jurisdictional boundaries. Water use metering and reporting requirements vary significantly between states. Satellite-based ET data could provide a nationally consistent approach to computing consumptive use of water applied for irrigation, and potentially for estimating the volume of water applied for crop irrigation, which is the largest source of consumptive water use in the US (Marston et al., 2018). However, these satellite-based irrigation calculations need to be comparable to what is actually happening on the ground, demonstrating the importance of high-fidelity in situ measurements of irrigation. This study was made possible by metered groundwater pumping records detailing the location, amount, and timing of irrigation. Outside of Kansas, metered records of irrigation are rare, with many states not requiring flowmeters on agricultural water uses (Marston, Abdallah, et al., 2022). This gap is increasingly being filled with reanalysis and ET-based water use products (Haynes et al., 2023; Martin et al., 2023). For ET-based irrigation data to become more useful to researchers, irrigators, regulators, and policymakers, metered irrigation records are needed for other areas with different soils, climate, irrigation practices, and cropping patterns to evaluate the performance of ET-based irrigation calculations under these different conditions.

The sources of uncertainty we discuss in Section 4.1 contributed to variable levels of agreement between ET-based and reported water withdrawals and applications across the comparisons we conducted. At the management area scale, we found a generally strong positive correlation (e.g., R^2 generally above 0.85; Table 1), comparable to other studies using remotely sensed data to estimate irrigation depths with statistical models (Filippelli et al., 2022; Majumdar et al., 2022; Wei et al., 2022). However, we observed a general positive bias and substantially more year-to-year variability in ET-based irrigation than in the reported data. The WRG and field scale comparisons had weaker correlations than the management area scale, in particular for irrigation depths, potentially indicating that irrigation depth predictions have greater uncertainty than irrigation volumes. However, across all scales, the agreement between ET-based irrigation calculations and reported data improved substantially when averaged over multiple years (Figure 3, Figure 5, Figure 7).

Since errors in estimated irrigation can lead to significant economic and hydrological impacts if used for management purposes (Foster et al., 2020), continued methodological development to overcome the uncertainties described above will be important to advance these tools for some applications. For instance, for purposes that require estimating long-term average consumptive use, such as calculating the water balance for a large (10s to 100s of km) region, the precipitation-adjusted spatially- and temporally-aggregated results we show in Figure 4 might be sufficient. In contrast, using these data for other purposes, such as monitoring within-season irrigation timing and volume from a specific well, would require significant improvements in the accuracy of calculated irrigation at these finer spatial and temporal scales and careful selection of an appropriate ET model. We found that statistical adjustments to ET-based irrigation calculations can substantially improve agreement with reported values at annual resolution (Figure 4b, Table S1), potentially suggesting a path towards greater local accuracy, and highlighting the critical importance of accurate effective precipitation values and ground-based data for comparison. While the approach we used required reported irrigation data, and therefore would not be tractable in locations without existing withdrawal monitoring, it may be possible to use a limited subset of reporting locations to develop relationships that can be applied more broadly (Bohling et al., 2021). Additional products, such as high-resolution soil moisture data from remote sensing-model integration (Vergopolan et al., 2021), may also provide a pathway for bias-correction and/or temporal disaggregation when integrated with field-specific water balance modeling tools (Hoekstra, 2019). Given that OpenET is a relatively new product (Melton et al., 2022), continued work on specific research and management applications will provide useful targets for prioritizing efforts to reduce existing uncertainties.

5. Conclusions

We evaluated the agreement between ET-based calculations of irrigation using a simple water balance approach and reported irrigation from a statewide database and farmer information. We found that there were generally positive correlations between the ET-based approaches and reported data, but that the ET-based approaches typically demonstrated more variability than reported values and overestimated irrigation, particularly during dry years. This may be partially attributed to changes in soil moisture storage and the approach used to calculate effective precipitation. We also found that agreement improved substantially when irrigation is averaged over multiple years, particularly at the field resolution where irrigated area was well-constrained. Key uncertainties were identified related to the choice of ET model and the approach used to map irrigation status and link wells to fields where irrigation water is used. The uncertainties in ET-based irrigation calculations likely exceed the signal of management activities in this region, suggesting further methodological refinement is needed for applications requiring precise quantification of irrigation depth for a given location and/or single year. However, for applications focused on relative differences in irrigation intensity across space and/or multi-year average irrigation applications, some of these uncertainties may safely be ignored. This work suggests that ET-based approaches to calculating irrigation are a potentially valuable approach for developing improved spatial and temporal water use data, and will likely require application-specific targeted improvements to reduce key uncertainties.

6. Acknowledgments

We appreciate assistance from Will Carrara and John Woods with data acquisition/processing and feedback on the manuscript from Sayantan Majumdar (Desert Research Institute). Ashley Grinstead's participation was supported by the Kansas Geological Survey Geohydrology Internship Program (https://www.kgs.ku.edu/Hydro/gipIndex.html). We greatly appreciate the farmers who were willing to share their water use data with us. This work was supported by National Aeronautics and Space Administration (NASA) [grant number 80NSSC22K1276] and National Science Foundation (NSF) [grant number RISE-2108196]. TF was also supported by Innovate UK [award number 10044695], as part of the UK Research and Innovation and European Commission funded project 'TRANSCEND: Transformational and robust adaptation to water scarcity and climate change under deep uncertainty'. Data and code used in the study are available at https://github.com/samzipper/SD-6_MapWaterConservation during the review process and will be posted to a repository with a DOI at the time of manuscript acceptance.

7. References

Abatzoglou, J. T. (2013). Development of gridded surface meteorological data for ecological applications and modelling. *International Journal of Climatology*, *33*(1), 121–131. https://doi.org/10.1002/joc.3413

Allen, R. G., Tasumi, M., Morse, A., & Trezza, R. (2005). A Landsat-based energy balance and evapotranspiration model in Western US water rights regulation and planning. *Irrigation and Drainage Systems*, *19*(3), 251–268. https://doi.org/10.1007/s10795-005-5187-z

Allen, R. G., Tasumi, M., Morse, A., Trezza, R., Wright, J. L., Bastiaanssen, W., et al. (2007). Satellite-based energy balance for mapping evapotranspiration with internalized calibration (METRIC)—Applications. *Journal of Irrigation and Drainage Engineering*, *133*(4), 395–406.

Allen, R. G., Pereira, L. S., Howell, T. A., & Jensen, M. E. (2011). Evapotranspiration information reporting: I. Factors governing measurement accuracy. *Agricultural Water Management*, *98*(6), 899–920. https://doi.org/10.1016/j.agwat.2010.12.015

Allen, R. G., Robison, C. W., Huntington, J., Wright, J. L., & Kilic, A. (2020). Applying the

FAO-56 dual Kc method for irrigation water requirements over large areas of the Western US. *Transactions of the ASABE*, *63*(6), 2059–2081. https://doi.org/10.13031/trans.13933

Anderson, M. C., Norman, J. M., Mecikalski, J. R., Otkin, J. A., & Kustas, W. P. (2007). A climatological study of evapotranspiration and moisture stress across the continental United States based on thermal remote sensing: 1. Model formulation. *Journal of Geophysical Research: Atmospheres*, *112*(D10). https://doi.org/10.1029/2006JD007506

Anderson, M. C., Gao, F., Knipper, K., Hain, C., Dulaney, W., Baldocchi, D., et al. (2018). Field-Scale Assessment of Land and Water Use Change over the California Delta Using Remote Sensing. *Remote Sensing*, *10*(6), 889. https://doi.org/10.3390/rs10060889

Bastiaanssen, W. G. M., Menenti, M., Feddes, R. A., & Holtslag, A. A. M. (1998). A remote sensing surface energy balance algorithm for land (SEBAL). 1. Formulation. *Journal of Hydrology*, *212*, 198–212.

Bohling, G. C., Butler, J. J., Whittemore, D. O., & Wilson, B. B. (2021). Evaluation of Data Needs for Assessments of Aquifers Supporting Irrigated Agriculture. *Water Resources Research*, *57*(4), e2020WR028320. https://doi.org/10.1029/2020WR028320

Brocca, L., Tarpanelli, A., Filippucci, P., Dorigo, W., Zaussinger, F., Gruber, A., & Fernández-Prieto, D. (2018). How much water is used for irrigation? A new approach exploiting coarse resolution satellite soil moisture products. *International Journal of Applied Earth Observation and Geoinformation*, *73*, 752–766. https://doi.org/10.1016/j.jag.2018.08.023

Brookfield, A. E., Zipper, S., Kendall, A. D., Ajami, H., & Deines, J. M. (2024). Estimating Groundwater Pumping for Irrigation: A Method Comparison. *Groundwater*, *62*(1), 15–33. https://doi.org/10.1111/gwat.13336

Butler, J. J., Whittemore, D. O., Wilson, B. B., & Bohling, G. C. (2016). A new approach for assessing the future of aquifers supporting irrigated agriculture. *Geophysical Research Letters*, *43*(5), 2004–2010. https://doi.org/10.1002/2016GL067879

Butler, J. J., Bohling, G. C., Whittemore, D. O., & Wilson, B. B. (2020). Charting Pathways Toward Sustainability for Aquifers Supporting Irrigated Agriculture. *Water Resources Research*, *56*(10), e2020WR027961. https://doi.org/10.1029/2020WR027961

Dalin, C., Wada, Y., Kastner, T., & Puma, M. J. (2017). Groundwater depletion embedded in international food trade. *Nature*, *543*(7647), 700–704. https://doi.org/10.1038/nature21403

Dari, J., Brocca, L., Quintana-Seguí, P., Escorihuela, M. J., Stefan, V., & Morbidelli, R. (2020). Exploiting High-Resolution Remote Sensing Soil Moisture to Estimate Irrigation Water Amounts over a Mediterranean Region. *Remote Sensing*, *12*(16), 2593. https://doi.org/10.3390/rs12162593

Deines, J. M., Kendall, A. D., Crowley, M. A., Rapp, J., Cardille, J. A., & Hyndman, D. W. (2019). Mapping three decades of annual irrigation across the US High Plains Aquifer using Landsat and Google Earth Engine. *Remote Sensing of Environment*, *233*, 111400. https://doi.org/10.1016/j.rse.2019.111400

Deines, J. M., Kendall, A. D., Butler, J. J., & Hyndman, D. W. (2019). Quantifying irrigation adaptation strategies in response to stakeholder-driven groundwater management in the US High Plains Aquifer. *Environmental Research Letters*, *14*(4), 044014. https://doi.org/10.1088/1748-9326/aafe39

Deines, J. M., Schipanski, M. E., Golden, B., Zipper, S. C., Nozari, S., Rottler, C., et al. (2020). Transitions from irrigated to dryland agriculture in the Ogallala Aquifer: Land use suitability and regional economic impacts. *Agricultural Water Management*, *233*, 106061. https://doi.org/10.1016/j.agwat.2020.106061

Deines, J. M., Kendall, A. D., Butler, J. J., Basso, B., & Hyndman, D. W. (2021). Combining Remote Sensing and Crop Models to Assess the Sustainability of Stakeholder-Driven Groundwater Management in the US High Plains Aquifer. *Water Resources Research*, e2020WR027756. https://doi.org/10.1029/2020WR027756

Dhungel, R., Aiken, R., Lin, X., Kenyon, S., Colaizzi, P. D., Luhman, R., et al. (2020). Restricted water allocations: Landscape-scale energy balance simulations and adjustments in agricultural water applications. *Agricultural Water Management*, *227*, 105854. https://doi.org/10.1016/j.agwat.2019.105854

D'Odorico, P., Carr, J., Dalin, C., Dell'Angelo, J., Konar, M., Laio, F., et al. (2019). Global virtual water trade and the hydrological cycle: patterns, drivers, and socio-environmental impacts. *Environmental Research Letters*, *14*(5), 053001. https://doi.org/10.1088/1748-9326/ab05f4

Drysdale, K. M., & Hendricks, N. P. (2018). Adaptation to an irrigation water restriction imposed through local governance. *Journal of Environmental Economics and Management*, *91*, 150–165. https://doi.org/10.1016/j.jeem.2018.08.002

Earnhart, D., & Hendricks, N. P. (2023). Adapting to water restrictions: Intensive versus extensive adaptation over time differentiated by water right seniority. *American Journal of Agricultural Economics*. https://doi.org/10.1111/ajae.12361

Feinstein, D. T., Fienen, M. N., Reeves, H. W., & Langevin, C. D. (2016). A Semi-Structured MODFLOW-USG Model to Evaluate Local Water Sources to Wells for Decision Support. *Groundwater*, *54*(4), 532–544. https://doi.org/10.1111/gwat.12389

Filippelli, S. K., Sloggy, M. R., Vogeler, J. C., Manning, D. T., Goemans, C., & Senay, G. B. (2022). Remote sensing of field-scale irrigation withdrawals in the central Ogallala aquifer region. *Agricultural Water Management*, *271*, 107764. https://doi.org/10.1016/j.agwat.2022.107764

Fisher, J. B., Tu, K. P., & Baldocchi, D. D. (2008). Global estimates of the land–atmosphere water flux based on monthly AVHRR and ISLSCP-II data, validated at 16 FLUXNET sites. *Remote Sensing of Environment*, *112*(3), 901–919. https://doi.org/10.1016/j.rse.2007.06.025

Folhes, M. T., Rennó, C. D., & Soares, J. V. (2009). Remote sensing for irrigation water management in the semi-arid Northeast of Brazil. *Agricultural Water Management*, *96*(10), 1398–1408. https://doi.org/10.1016/j.agwat.2009.04.021

Foster, T., Gonçalves, I. Z., Campos, I., Neale, C. M. U., & Brozović, N. (2019). Assessing landscape scale heterogeneity in irrigation water use with remote sensing and in situ monitoring. *Environmental Research Letters*, *14*(2), 024004. https://doi.org/10.1088/1748-9326/aaf2be

Foster, T., Mieno, T., & Brozović, N. (2020). Satellite-Based Monitoring of Irrigation Water Use: Assessing Measurement Errors and Their Implications for Agricultural Water Management Policy. *Water Resources Research*, *56*(11), e2020WR028378. https://doi.org/10.1029/2020WR028378

Gao, J., Sheshukov, A. Y., Yen, H., Kastens, J. H., & Peterson, D. L. (2017). Impacts of incorporating dominant crop rotation patterns as primary land use change on hydrologic model performance. *Agriculture, Ecosystems & Environment*, *247*, 33–42. https://doi.org/10.1016/j.agee.2017.06.019

Gibson, J., Franz, T. E., Wang, T., Gates, J., Grassini, P., Yang, H., & Eisenhauer, D. (2017). A case study of field-scale maize irrigation patterns in western Nebraska: implications for water managers and recommendations for hyper-resolution land surface modeling. *Hydrology and Earth System Sciences*, *21*(2), 1051–1062. https://doi.org/10.5194/hess-21-1051-2017

Gleeson, T., Cuthbert, M., Ferguson, G., & Perrone, D. (2020). Global Groundwater Sustainability, Resources, and Systems in the Anthropocene. *Annual Review of Earth and Planetary Sciences*, *48*(1). https://doi.org/10.1146/annurev-earth-071719-055251

Glose, T. J., Zipper, S., Hyndman, D. W., Kendall, A. D., Deines, J. M., & Butler, J. J. (2022). Quantifying the impact of lagged hydrological responses on the effectiveness of groundwater conservation. *Water Resources Research*, *58*(7), e2022WR032295. https://doi.org/10.1029/2022WR032295

Golden, B. (2018). *Monitoring the Impacts of Sheridan County 6 Local Enhanced Management Area*. Kansas State University. Retrieved from https://agriculture.ks.gov/docs/default-source/dwr-water-appropriation-documents/sheridancounty6_lema_goldenreport_2013-2017.pdf?sfvrsn=dac48ac1_0

de Graaf, I. E. M., Gleeson, T., Beek, L. P. H. (Rens) van, Sutanudjaja, E. H., & Bierkens, M. F. P. (2019). Environmental flow limits to global groundwater pumping. *Nature*, *574*(7776), 90–94. https://doi.org/10.1038/s41586-019-1594-4

Hasan, M. F., Smith, R., Vajedian, S., Pommerenke, R., & Majumdar, S. (2023). Global land subsidence mapping reveals widespread loss of aquifer storage capacity. *Nature Communications*, *14*(1), 6180. https://doi.org/10.1038/s41467-023-41933-z

Haynes, J. V., Read, A. L., Chan, A. Y., Martin, D. J., Regan, R. S., Henson, W., et al. (2023). Monthly crop irrigation withdrawals and efficiencies by HUC12 watershed for years 2000-2020 within the conterminous United States [Data set]. U.S. Geological Survey. https://doi.org/10.5066/P9LGISUM

Hoekstra, A. Y. (2019). Green-blue water accounting in a soil water balance. *Advances in Water Resources*, *129*, 112–117. https://doi.org/10.1016/j.advwatres.2019.05.012

Jalilvand, E., Tajrishy, M., Ghazi Zadeh Hashemi, S. A., & Brocca, L. (2019). Quantification of irrigation water using remote sensing of soil moisture in a semi-arid region. *Remote Sensing of Environment*, *231*, 111226. https://doi.org/10.1016/j.rse.2019.111226

Jasechko, S., Seybold, H., Perrone, D., Fan, Y., Shamsudduha, M., Taylor, R. G., et al. (2024). Rapid groundwater decline and some cases of recovery in aquifers globally. *Nature*, *625*(7996), 715–721. https://doi.org/10.1038/s41586-023-06879-8

Ketchum, D., Hoylman, Z. H., Huntington, J., Brinkerhoff, D., & Jencso, K. G. (2023). Irrigation intensification impacts sustainability of streamflow in the Western United States. *Communications Earth & Environment*, *4*(1), 1–8. https://doi.org/10.1038/s43247-023-01152-2

Kharrou, M. H., Simonneaux, V., Er-Raki, S., Le Page, M., Khabba, S., & Chehbouni, A. (2021). Assessing Irrigation Water Use with Remote Sensing-Based Soil Water Balance at an Irrigation Scheme Level in a Semi-Arid Region of Morocco. *Remote Sensing*, *13*(6), 1133. https://doi.org/10.3390/rs13061133

Kniffin, M., Bradbury, K. R., Fienen, M., & Genskow, K. (2020). Groundwater Model Simulations of Stakeholder-Identified Scenarios in a High-Conflict Irrigated Area. *Groundwater*, *58*(6), 973–986. https://doi.org/10.1111/gwat.12989

Laipelt, L., Henrique Bloedow Kayser, R., Santos Fleischmann, A., Ruhoff, A., Bastiaanssen, W., Erickson, T. A., & Melton, F. (2021). Long-term monitoring of evapotranspiration using the SEBAL algorithm and Google Earth Engine cloud computing. *ISPRS Journal of Photogrammetry and Remote Sensing*, *178*, 81–96. https://doi.org/10.1016/j.isprsjprs.2021.05.018

Lamb, S. E., Haacker, E. M. K., & Smidt, S. J. (2021). Influence of Irrigation Drivers Using Boosted Regression Trees: Kansas High Plains. *Water Resources Research*, *57*(5), e2020WR028867. https://doi.org/10.1029/2020WR028867

Majumdar, S., Smith, R., Conway, B. D., & Lakshmi, V. (2022). Advancing remote sensing and machine learning-driven frameworks for groundwater withdrawal estimation in Arizona: Linking land subsidence to groundwater withdrawals. *Hydrological Processes*, *36*(11), e14757. https://doi.org/10.1002/hyp.14757

MardanDoost, B., Brookfield, A. E., Feddema, J., Sturm, B., Kastens, J., Peterson, D., & Bishop, C. (2019). Estimating irrigation demand with geospatial and in-situ data: Application to the high plains aquifer, Kansas, USA. *Agricultural Water Management*, *223*, 105675. https://doi.org/10.1016/j.agwat.2019.06.010

Marston, L. T., Ao, Y., Konar, M., Mekonnen, M. M., & Hoekstra, A. Y. (2018). High-Resolution Water Footprints of Production of the United States. *Water Resources Research*, *54*(3), 2288–2316. https://doi.org/10.1002/2017WR021923

Marston, L. T., Lamsal, G., Ancona, Z. H., Caldwell, P., Richter, B. D., Ruddell, B. L., et al. (2020). Reducing water scarcity by improving water productivity in the United States. *Environmental Research Letters*, *15*(9), 094033. https://doi.org/10.1088/1748-9326/ab9d39

Marston, L. T., Zipper, S., Smith, S. M., Allen, J. J., Butler, J. J., Gautam, S., & Yu, D. J. (2022). The importance of fit in groundwater self-governance. *Environmental Research Letters*, *17*(11), 111001. https://doi.org/10.1088/1748-9326/ac9a5e

Marston, L. T., Abdallah, A. M., Bagstad, K. J., Dickson, K., Glynn, P., Larsen, S. G., et al. (2022). Water-Use Data in the United States: Challenges and Future Directions. *JAWRA Journal of the American Water Resources Association*, *58*(4), 485–495. https://doi.org/10.1111/1752-1688.13004

Martin, D., Regan, R. S., Haynes, J. V., Read, A. L., Henson, W., Stewart, J. S., et al. (2023). Irrigation water use reanalysis for the 2000-20 period by HUC12, month, and year for the conterminous United States [Data set]. U.S. Geological Survey. https://doi.org/10.5066/P9YWR0OJ

Melton, F. S., Johnson, L. F., Lund, C. P., Pierce, L. L., Michaelis, A. R., Hiatt, S. H., et al. (2012). Satellite Irrigation Management Support With the Terrestrial Observation and Prediction System: A Framework for Integration of Satellite and Surface Observations to Support Improvements in Agricultural Water Resource Management. *IEEE Journal of Selected Topics in Applied Earth Observations and Remote Sensing*, *5*(6), 1709–1721. https://doi.org/10.1109/JSTARS.2012.2214474

Melton, F. S., Huntington, J., Grimm, R., Herring, J., Hall, M., Rollison, D., et al. (2022). OpenET: Filling a Critical Data Gap in Water Management for the Western United States. *JAWRA Journal of the American Water Resources Association*, *58*(6), 971–994. https://doi.org/10.1111/1752-1688.12956

Mourtzinis, S., Rattalino Edreira, J. I., Conley, S. P., & Grassini, P. (2017). From grid to field: Assessing quality of gridded weather data for agricultural applications. *European Journal of Agronomy*, *82*, 163–172. https://doi.org/10.1016/j.eja.2016.10.013

Ott, T. J., Majumdar, S., Huntington, J., Pearson, C., Bromley, M., Minor, B. A., et al. (2024). Toward Sustainable Groundwater Management: Harnessing Remote Sensing and Climate Data to Estimate Field-Scale Groundwater Pumping. *ESS Open Archive*. https://doi.org/10.22541/essoar.170800918.86740881/v1

Pereira, L. S., Paredes, P., Melton, F., Johnson, L., Wang, T., López-Urrea, R., et al. (2020). Prediction of crop coefficients from fraction of ground cover and height. Background and validation using ground and remote sensing data. *Agricultural Water Management*, *241*, 106197. https://doi.org/10.1016/j.agwat.2020.106197

Pereira, L. S., Paredes, P., & Jovanovic, N. (2020). Soil water balance models for determining crop water and irrigation requirements and irrigation scheduling focusing on the FAO56 method and the dual Kc approach. *Agricultural Water Management*, *241*, 106357. https://doi.org/10.1016/j.agwat.2020.106357

Peterson, T. J., & Fulton, S. (2019). Joint Estimation of Gross Recharge, Groundwater Usage, and Hydraulic Properties within HydroSight. *Groundwater*, *57*(6), 860–876. https://doi.org/10.1111/gwat.12946

Senay, G. B., Friedrichs, M., Morton, C., Parrish, G. E. L., Schauer, M., Khand, K., et al. (2022). Mapping actual evapotranspiration using Landsat for the conterminous United States: Google Earth Engine implementation and assessment of the SSEBop model. *Remote Sensing of Environment*, *275*, 113011. https://doi.org/10.1016/j.rse.2022.113011

Steiner, J. L., Devlin, D. L., Perkins, S., Aguilar, J. P., Golden, B., Santos, E. A., & Unruh, M. (2021). Policy, Technology, and Management Options for Water Conservation in the Ogallala Aquifer in Kansas, USA. *Water*, *13*(23), 3406. https://doi.org/10.3390/w13233406

Tolley, D., Foglia, L., & Harter, T. (2019). Sensitivity Analysis and Calibration of an Integrated Hydrologic Model in an Irrigated Agricultural Basin With a Groundwater-Dependent Ecosystem. *Water Resources Research*, *55*(9), 7876–7901. https://doi.org/10.1029/2018WR024209

USDA. (2022). *Cropland Data Layer [Online]*. Washington, D.C.: USDA National Agricultural Statistics Service. Retrieved from https://nassgeodata.gmu.edu/CropScape/

Vergopolan, N., Chaney, N. W., Pan, M., Sheffield, J., Beck, H. E., Ferguson, C. R., et al. (2021). SMAP-HydroBlocks, a 30-m satellite-based soil moisture dataset for the conterminous US. *Scientific Data*, *8*(1), 264. https://doi.org/10.1038/s41597-021-01050-2

Volk, J. M., Huntington, J. L., Melton, F. S., Allen, R., Anderson, M., Fisher, J. B., et al. (2024). Assessing the accuracy of OpenET satellite-based evapotranspiration data to support water resource and land management applications. *Nature Water*, 1–13. https://doi.org/10.1038/s44221-023-00181-7

Wei, S., Xu, T., Niu, G.-Y., & Zeng, R. (2022). Estimating Irrigation Water Consumption Using Machine Learning and Remote Sensing Data in Kansas High Plains. *Remote Sensing*, *14*(13), 3004. https://doi.org/10.3390/rs14133004

Whittemore, D. O., Butler, J. J., Bohling, G. C., & Wilson, B. B. (2023). Are we saving water? Simple methods for assessing the effectiveness of groundwater conservation measures. *Agricultural Water Management*, *287*, 108408. https://doi.org/10.1016/j.agwat.2023.108408

Wilson, B. B., Liu, G., Bohling, G. C., & Butler, J. J. (2021). *GMD4 Groundwater Flow Model: High Plains Aquifer Modeling Maintenance Project* (KGS Open File Report 2021-6). Lawrence KS.

Xu, T., Deines, J. M., Kendall, A. D., Basso, B., & Hyndman, D. W. (2019). Addressing Challenges for Mapping Irrigated Fields in Subhumid Temperate Regions by Integrating Remote Sensing and Hydroclimatic Data. *Remote Sensing*, *11*(3), 370. https://doi.org/10.3390/rs11030370

Zipper, S. C., Stack Whitney, K., Deines, J. M., Befus, K. M., Bhatia, U., Albers, S. J., et al. (2019). Balancing Open Science and Data Privacy in the Water Sciences. *Water Resources Research*, *55*(7), 5202–5211. https://doi.org/10.1029/2019WR025080

Zipper, S. C., Carah, J. K., Dillis, C., Gleeson, T., Kerr, B., Rohde, M. M., et al. (2019). Cannabis and residential groundwater pumping impacts on streamflow and ecosystems in Northern California. *Environmental Research Communications*, *1*(12), 125005. https://doi.org/10.1088/2515-7620/ab534d

Zipper, S. C., Gleeson, T., Li, Q., & Kerr, B. (2021). Comparing Streamflow Depletion Estimation Approaches in a Heavily Stressed, Conjunctively Managed Aquifer. *Water Resources Research*, *57*(2), e2020WR027591. https://doi.org/10.1029/2020WR027591

Zipper, S. C., Farmer, W. H., Brookfield, A., Ajami, H., Reeves, H. W., Wardropper, C., et al. (2022). Quantifying Streamflow Depletion from Groundwater Pumping: A Practical Review of Past and Emerging Approaches for Water Management. *JAWRA Journal of the American Water Resources Association*, *58*(2), 289–312. https://doi.org/10.1111/1752-1688.12998

Supplemental material for:

Estimating irrigation water use from remotely sensed evapotranspiration data: Accuracy and uncertainties across spatial scales

Authors: Sam Zipper[1,2,*], Jude Kastens[3], Timothy Foster[4], Brownie Wilson[1], Forrest Melton[5], Ashley Grinstead[1,6], Jillian M. Deines[7], James J. Butler[1], Landon T. Marston[8]

Affiliations:

1. Kansas Geological Survey, University of Kansas, Lawrence KS 66047
2. Department of Geology, University of Kansas, Lawrence KS 66045
3. Kansas Biological Survey & Center for Ecological Research, University of Kansas, Lawrence KS 66047
4. School of Engineering, University of Manchester, Manchester, UK
5. Atmospheric Science Branch, Earth Science Division, NASA Ames Research Center, Moffett Field, CA 94035
6. Department of Natural Resources and the Environment, University of Connecticut, Storrs, CT 06269, United States
7. Earth Systems Predictability and Resiliency Group, Pacific Northwest National Laboratory, Richland, WA 99354
8. Department of Civil and Environmental Engineering, Virginia Tech, Blacksburg VA 24061

*Correspondence to samzipper@ku.edu

Section SI1. Additional information about the study area.

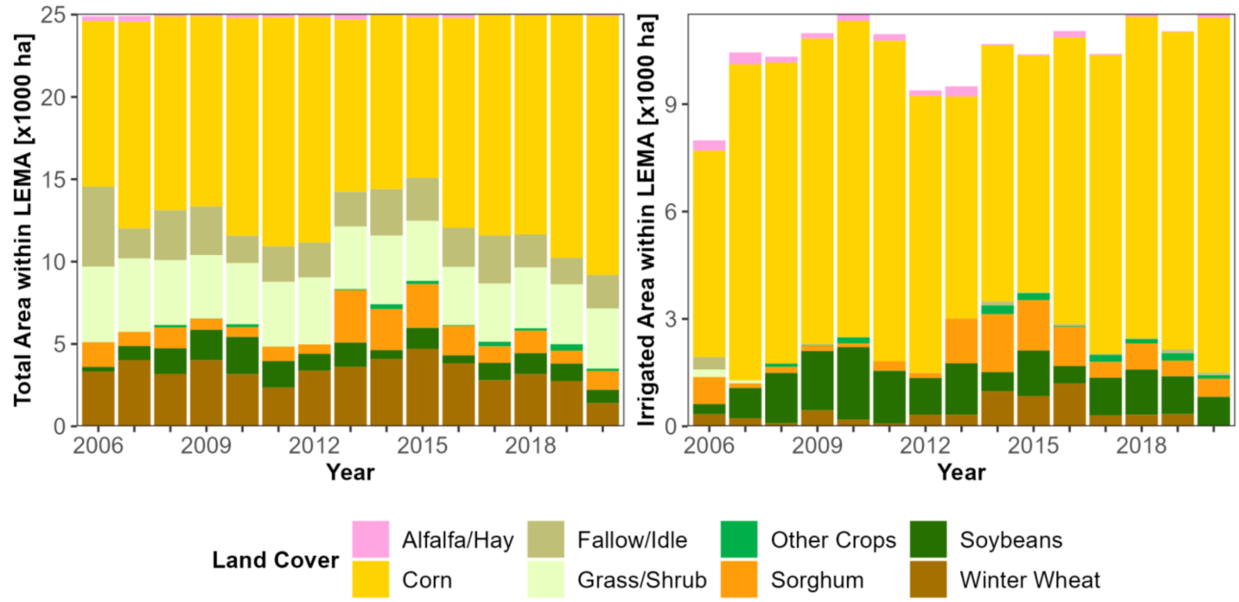

Figure S1. Annual area within LEMA for each land cover for all fields (left) and irrigated fields (right), from the USDA Cropland Data Layer. Irrigated fields were identified using AIM (Deines, Kendall, Crowley, et al., 2019).

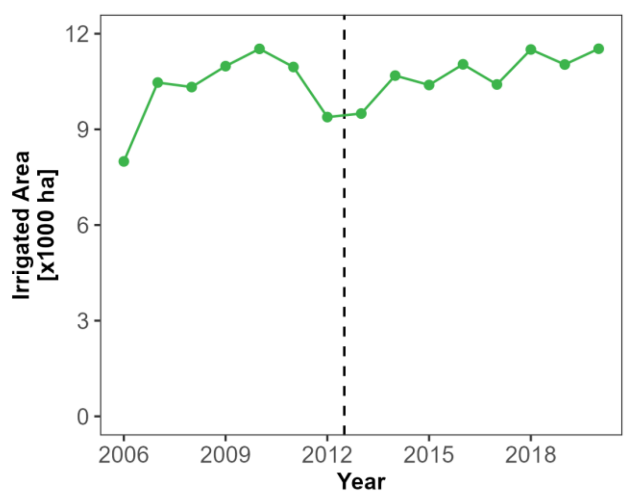

Figure S2. Annual irrigated area within the SD-6 LEMA from 2006 to 2021, based on AIM (Deines, Kendall, Crowley, et al., 2019). The dashed line shows the onset of the SD-6 LEMA.

Section SI2. Additional plots related to irrigation calculations in the SD-6 LEMA area.

Table S1. Fit statistics for precipitation-corrected calculated irrigation shown in Figure 4b.

Model	**MAE [x10^7 m^3]**	**Bias [%]**	**Slope**	**R^2**
Ensemble	0.093	0	1.01	0.95
DisALEXI	0.341	0	0.56	0.46
eeMETRIC	0.169	0	0.97	0.85
geeSEBAL	0.184	0	0.85	0.78
PT-JPL	0.122	0	0.96	0.90
SIMS	0.100	0	1.02	0.95
SSEBop	0.132	0	0.96	0.89

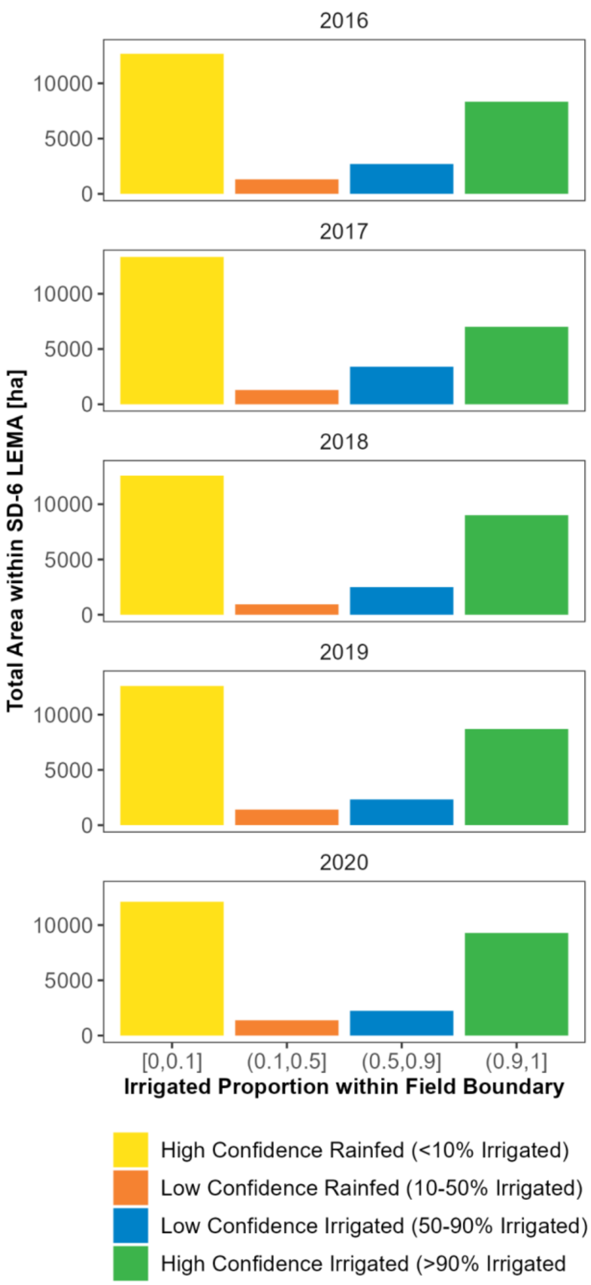

Figure S3. Characterization of confidence in irrigation classification and field boundary by year for the SD-6 LEMA area. The y-axis shows the total area in each of the 4 bins. The “High Confidence Rainfed” and “High Confidence Irrigated” fields have <10% and >90% of pixels within the field boundary mapped as irrigated by AIM, respectively. The “Low Confidence Rainfed” and “Low Confidence Irrigated” are classified as rainfed and irrigated, respectively, but have a larger >10% of the pixels within the field mapped as the opposite practice. Across all years, there is more Low Confidence Irrigated land than Low Confidence Rainfed land, suggesting that any errors in irrigation classification are likely to bias irrigated area high relative to reported data.

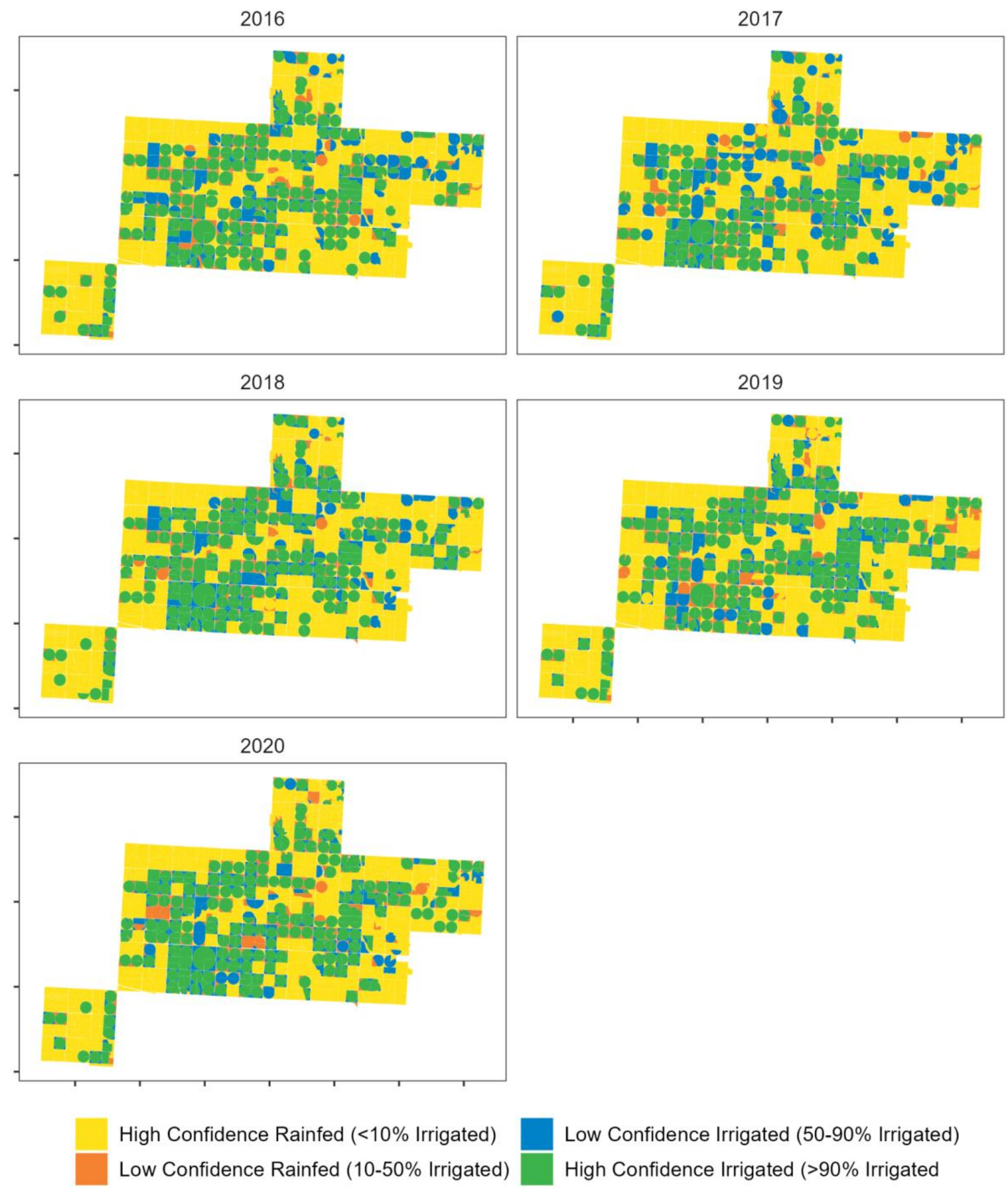

Figure S4. Map showing spatial distribution of irrigated classification and field boundary confidence data shown in Figure S3.

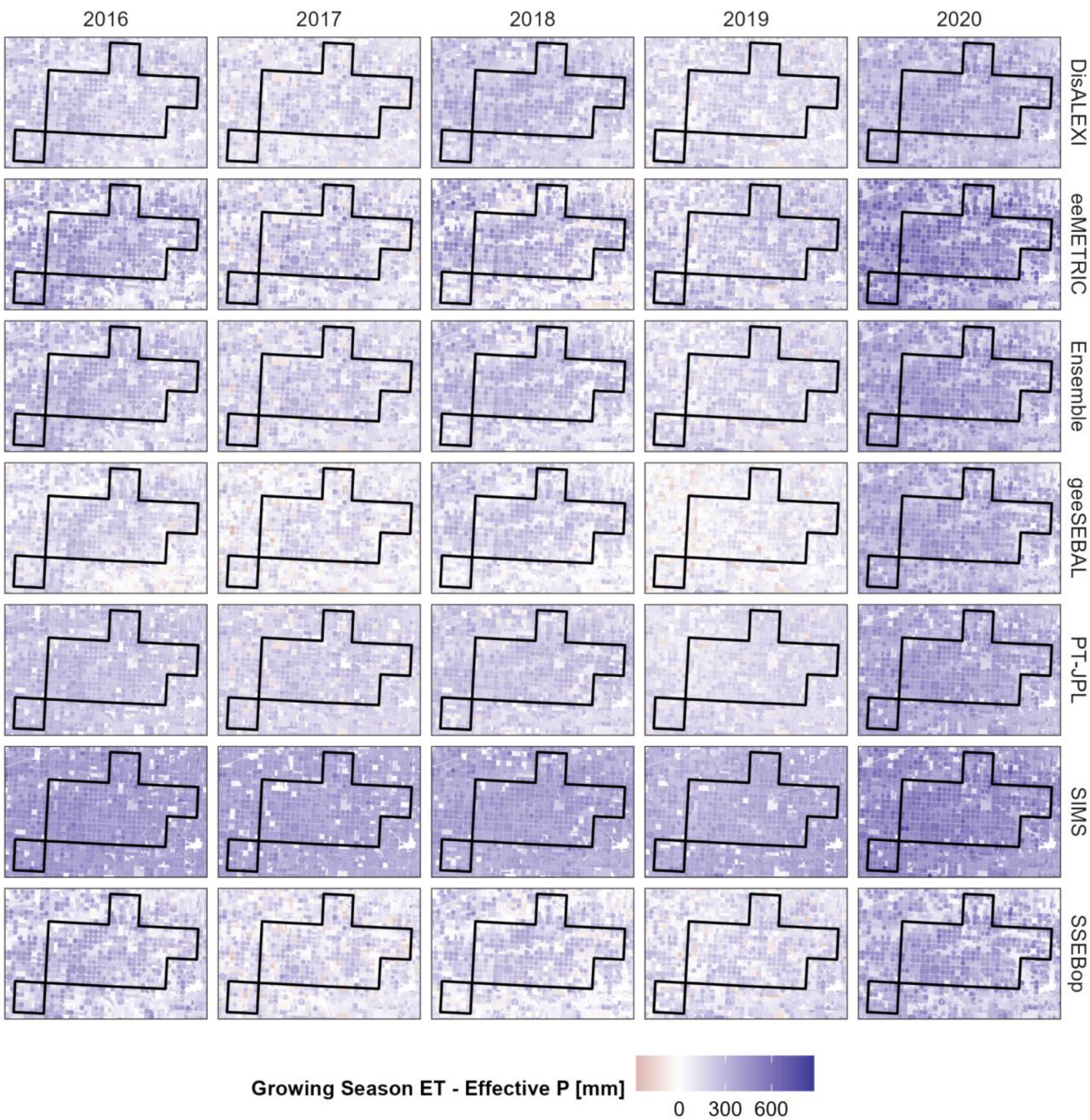

Figure S5. Maps of estimated field-resolution ET - effective precipitation for each year and model. The black outline corresponds to the SD-6 LEMA.

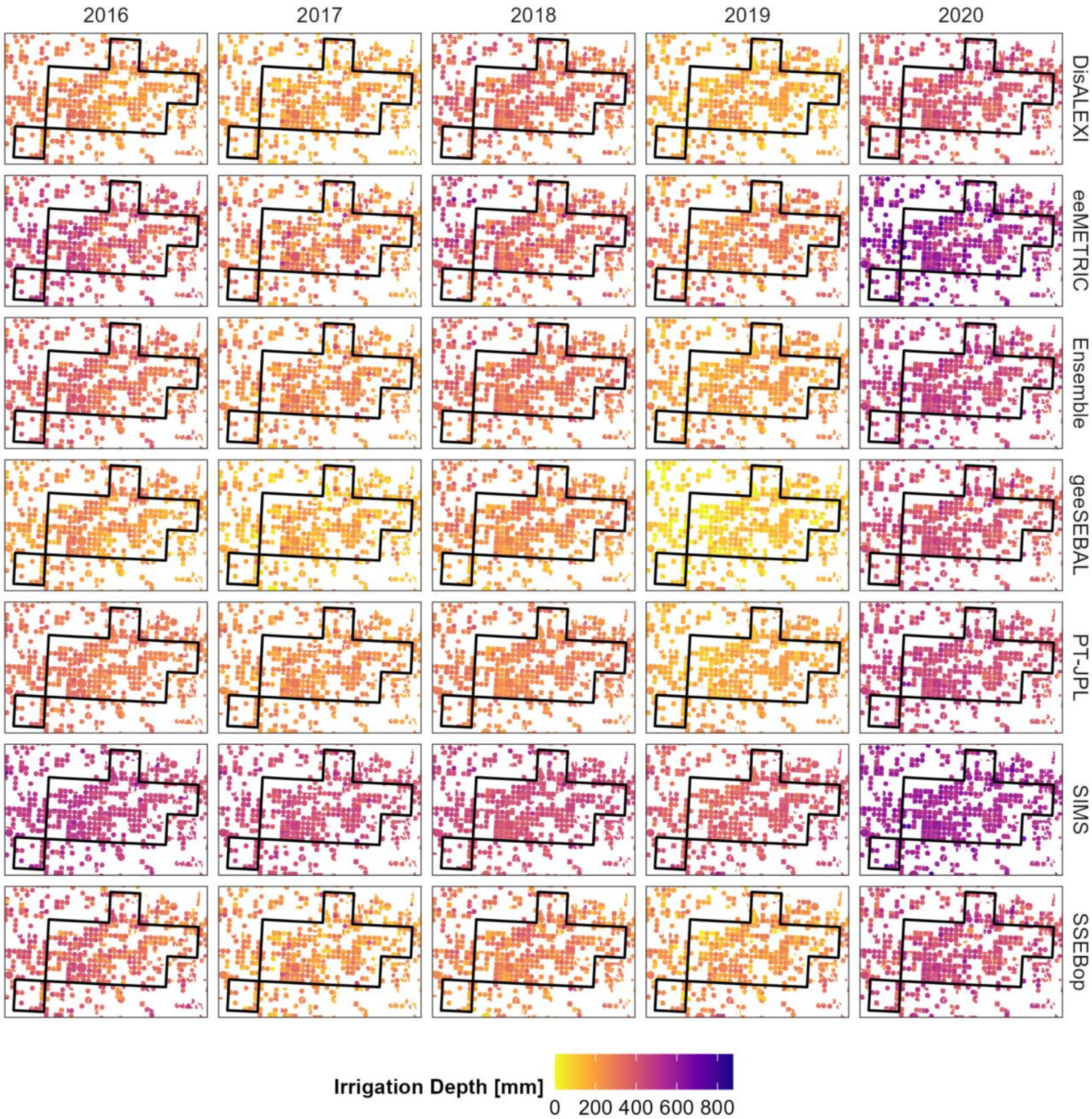

Figure S6. Maps of estimated field-resolution irrigation for each year and model. Fields that are classified as non-irrigated are not shown. The black outline corresponds to the SD-6 LEMA.

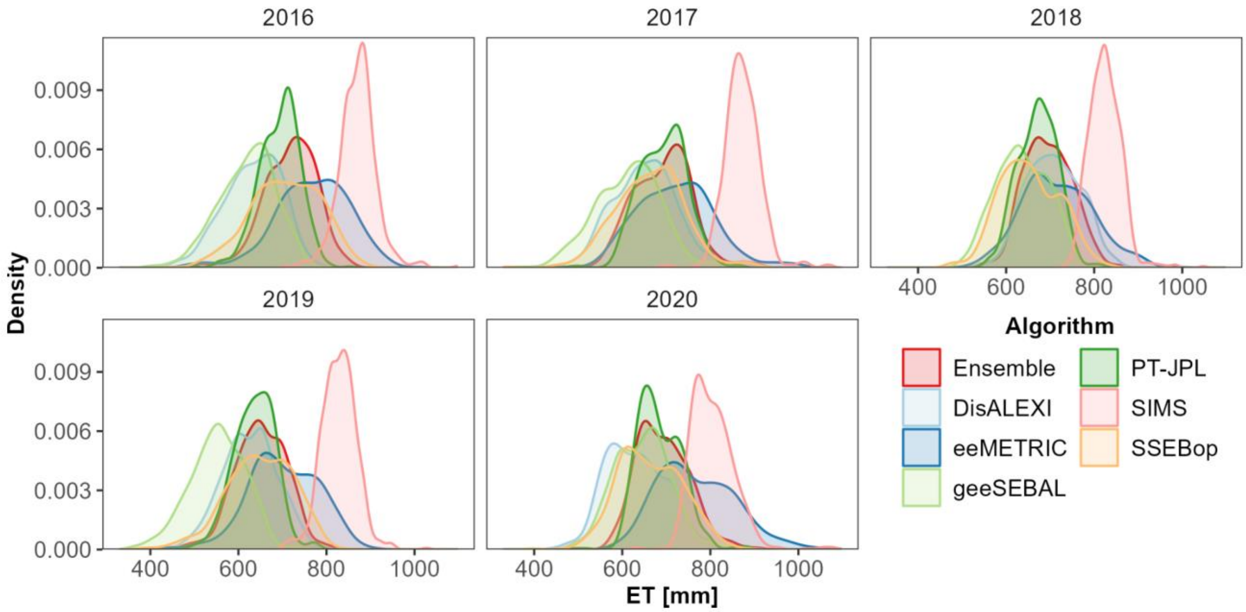

Figure S7. Density plots of field-resolution ET for irrigated fields in the SD-6 LEMA by year.

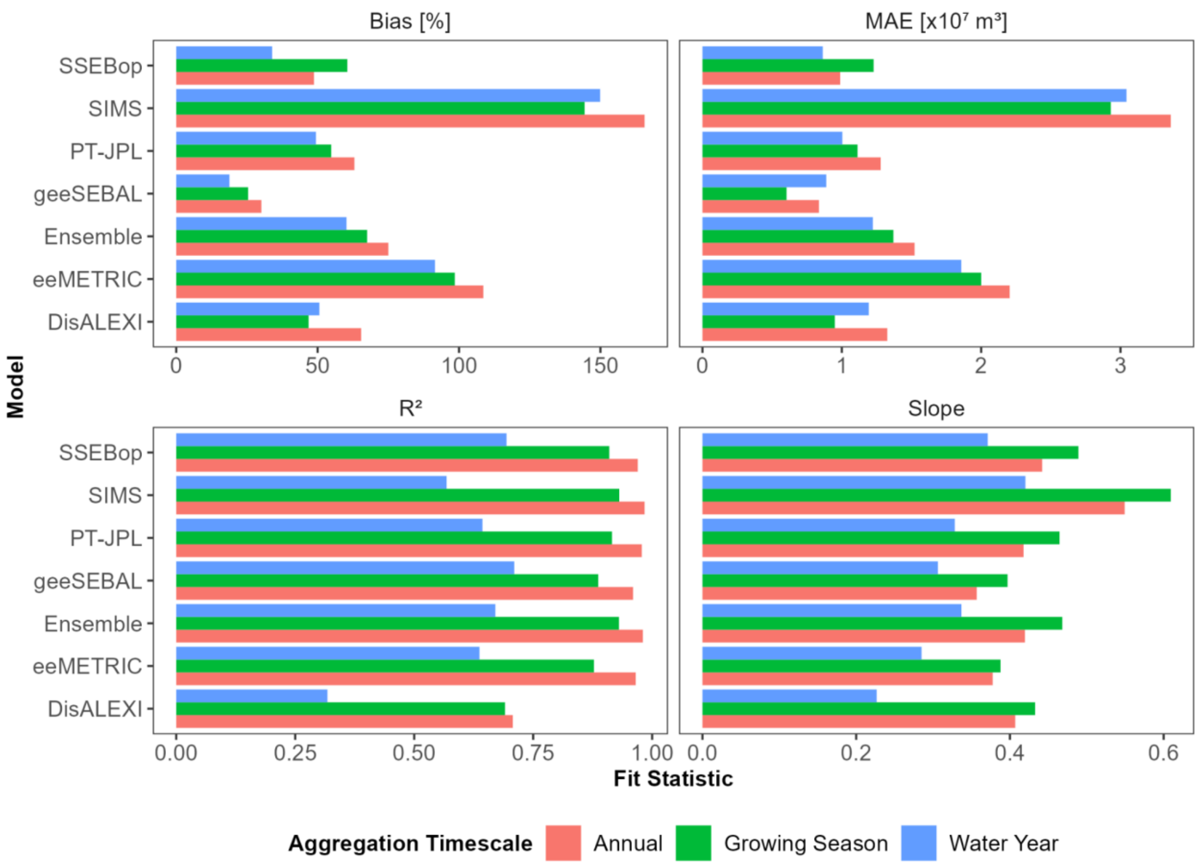

Figure S8. Summary of fit statistics for comparison between each OpenET model and WIMAS data for total LEMA-scale pumping (i.e., data from Table 1 in graphical form).

Section SI3. Additional plots related to effective precipitation use in irrigation calculations

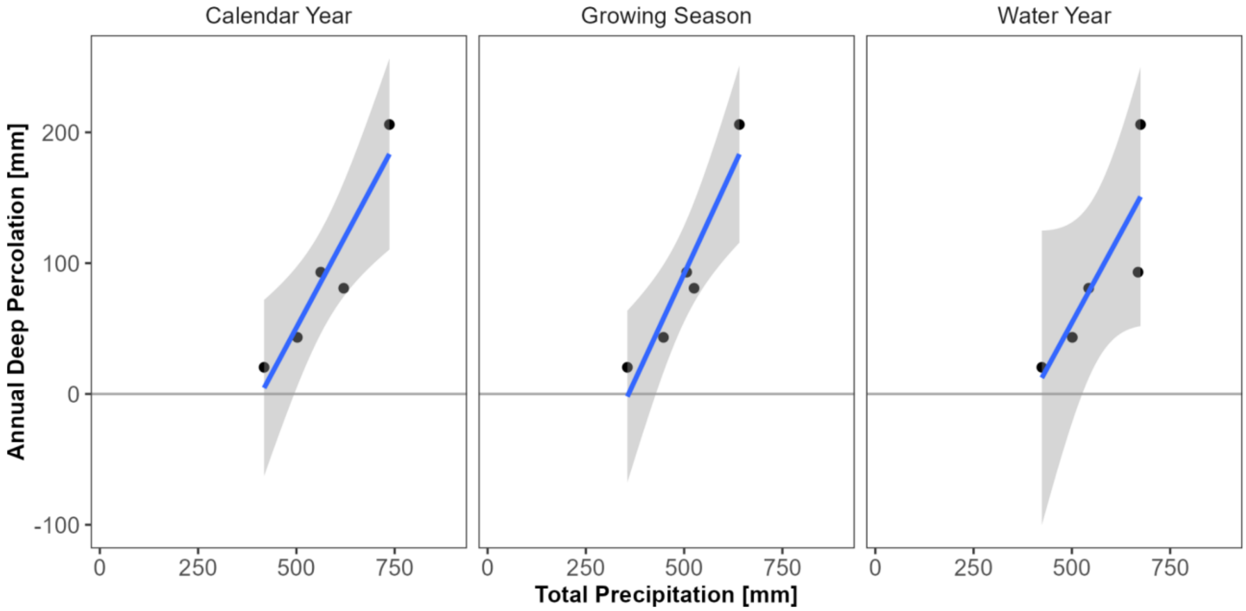

Figure S9. Relationship between deep percolation (from 2013-2017 simulated data from Deines et al., 2021) and calendar year, growing season, and water year total precipitation. Blue line shows linear best fit relationship and standard error in each plot.

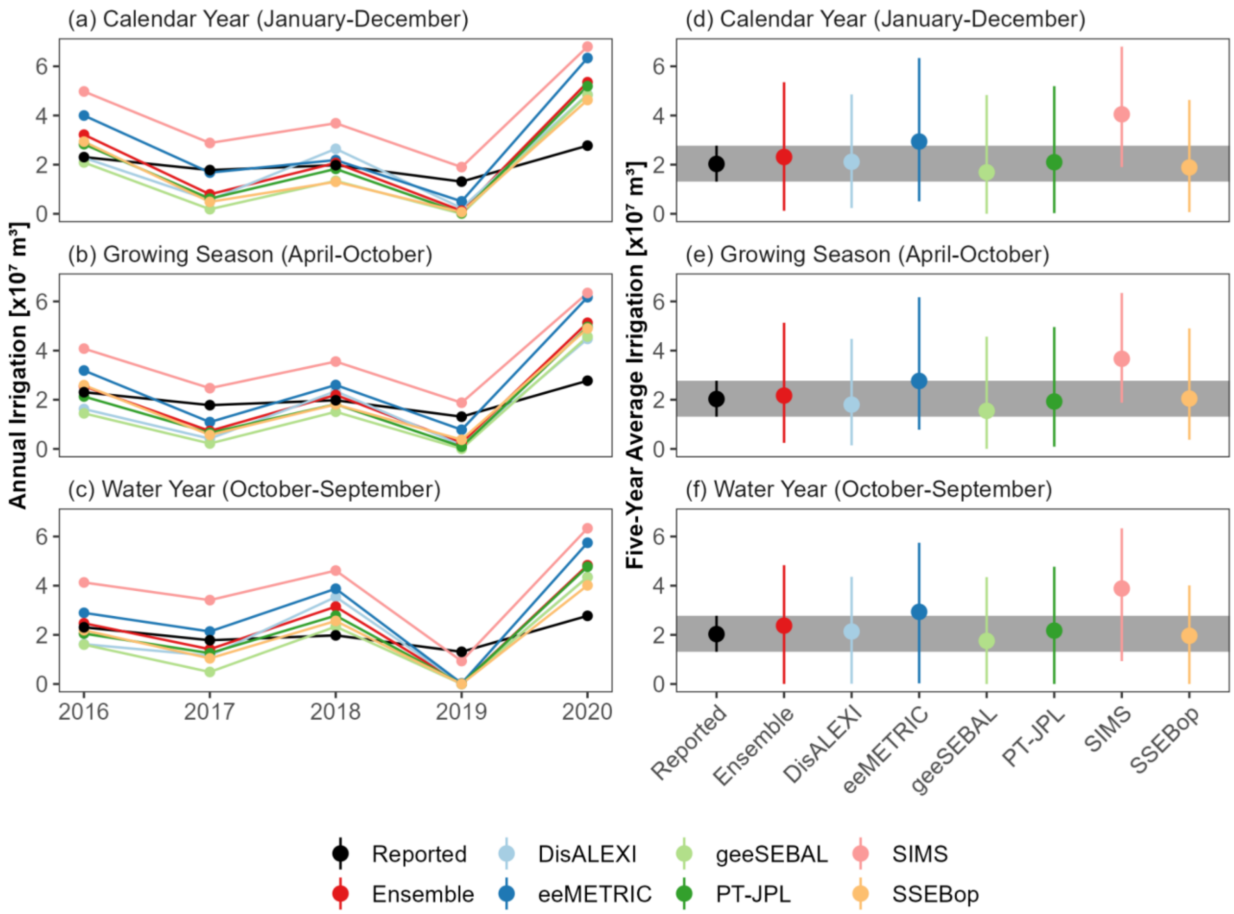

Figure S10. Same as Figure 3, but using precipitation in irrigation calculations instead of effective precipitation.

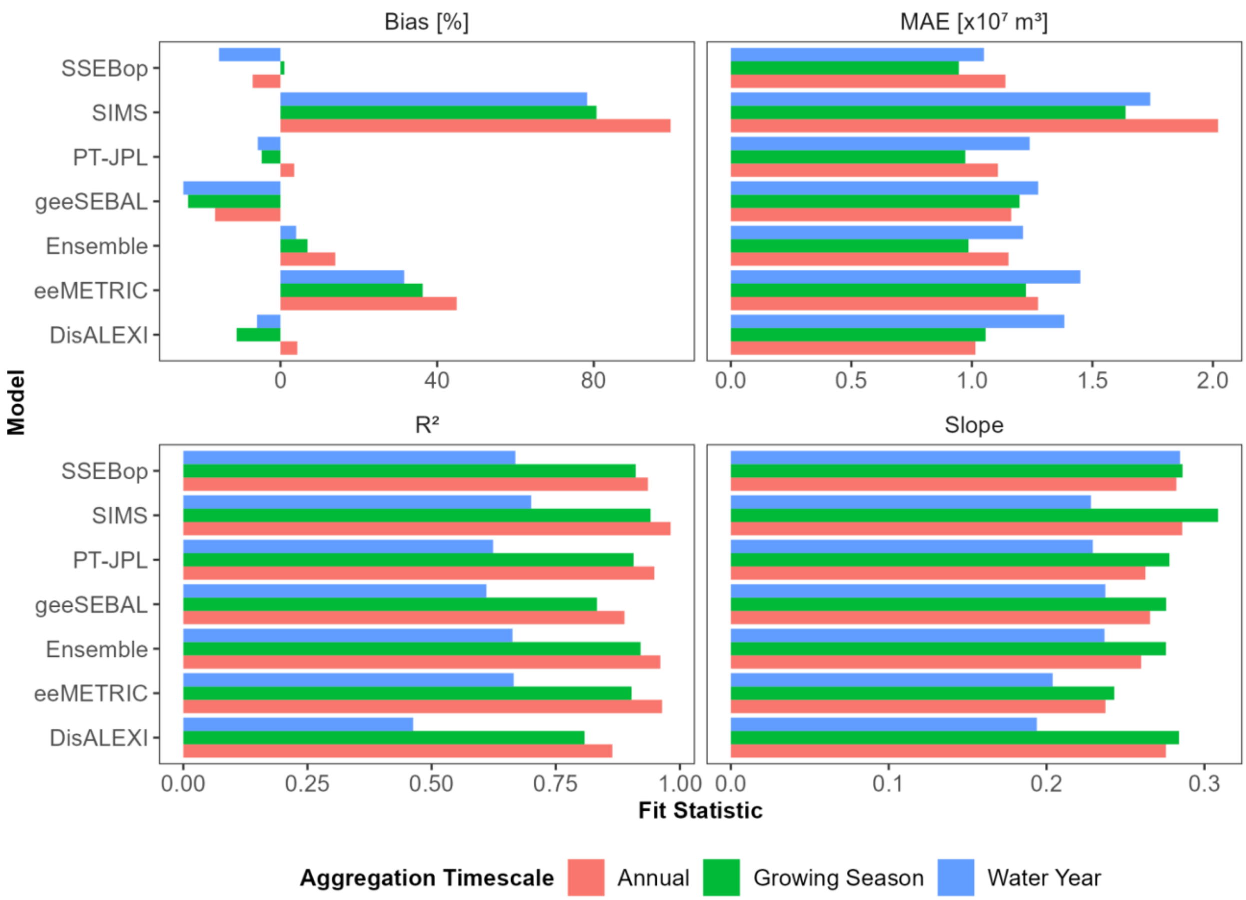

1056
1057 Figure S11. Same as Figure S8, but using precipitation in irrigation calculations instead of
1058 effective precipitation.
1059

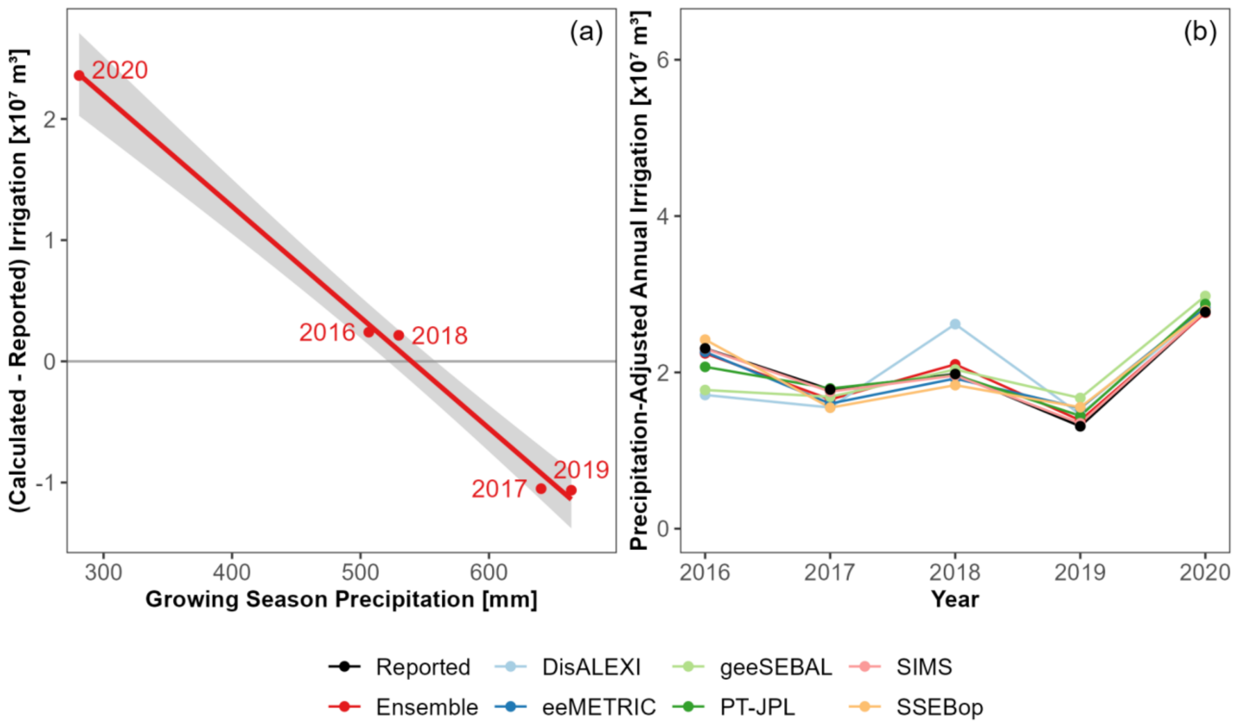

Figure S12. Same as Figure 4, but using precipitation in irrigation calculations instead of effective precipitation.

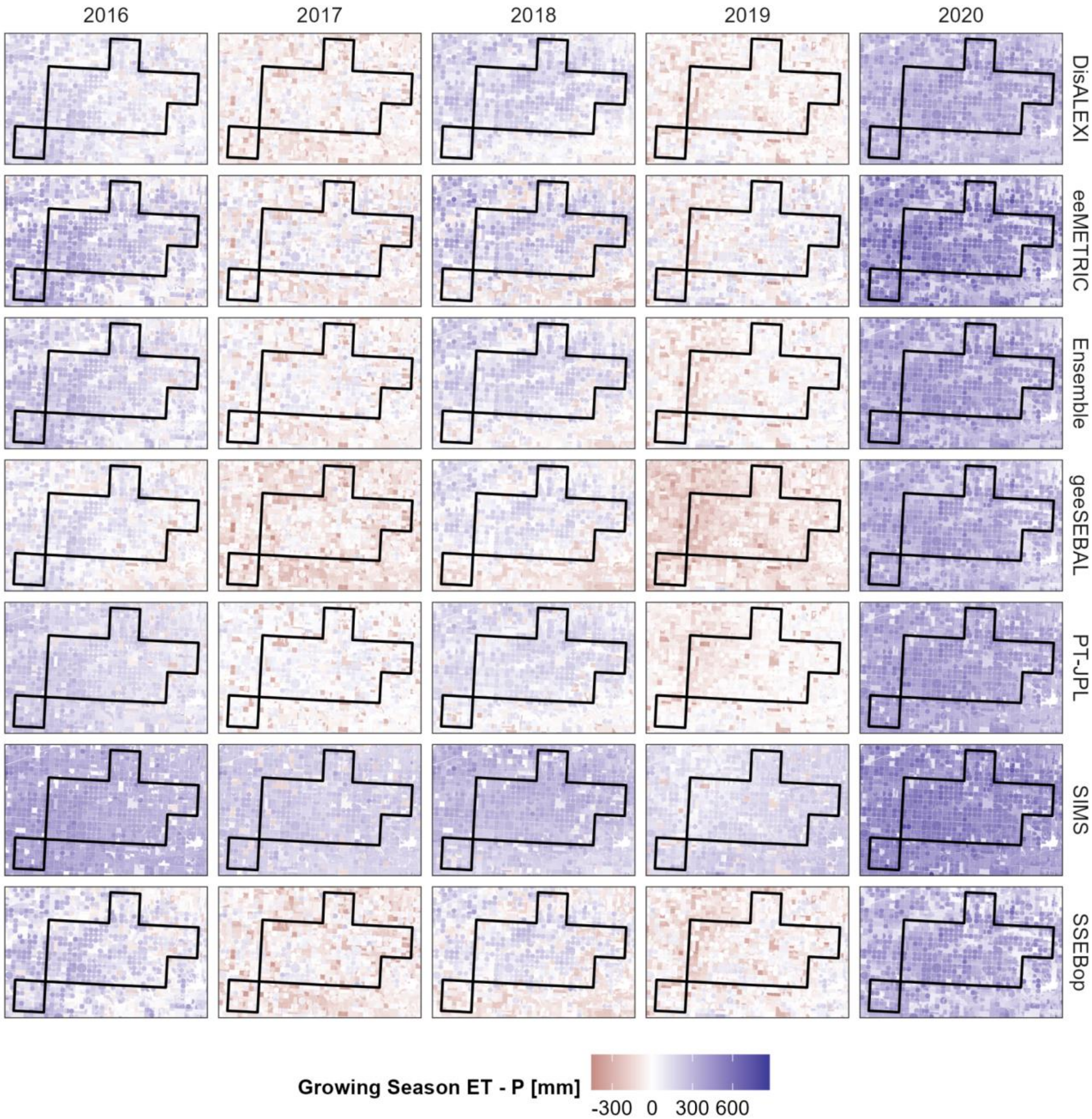

1064
1065 Figure S13. Same as Figure S5, but using total growing season precipitation instead of effective
1066 precipitation.
1067

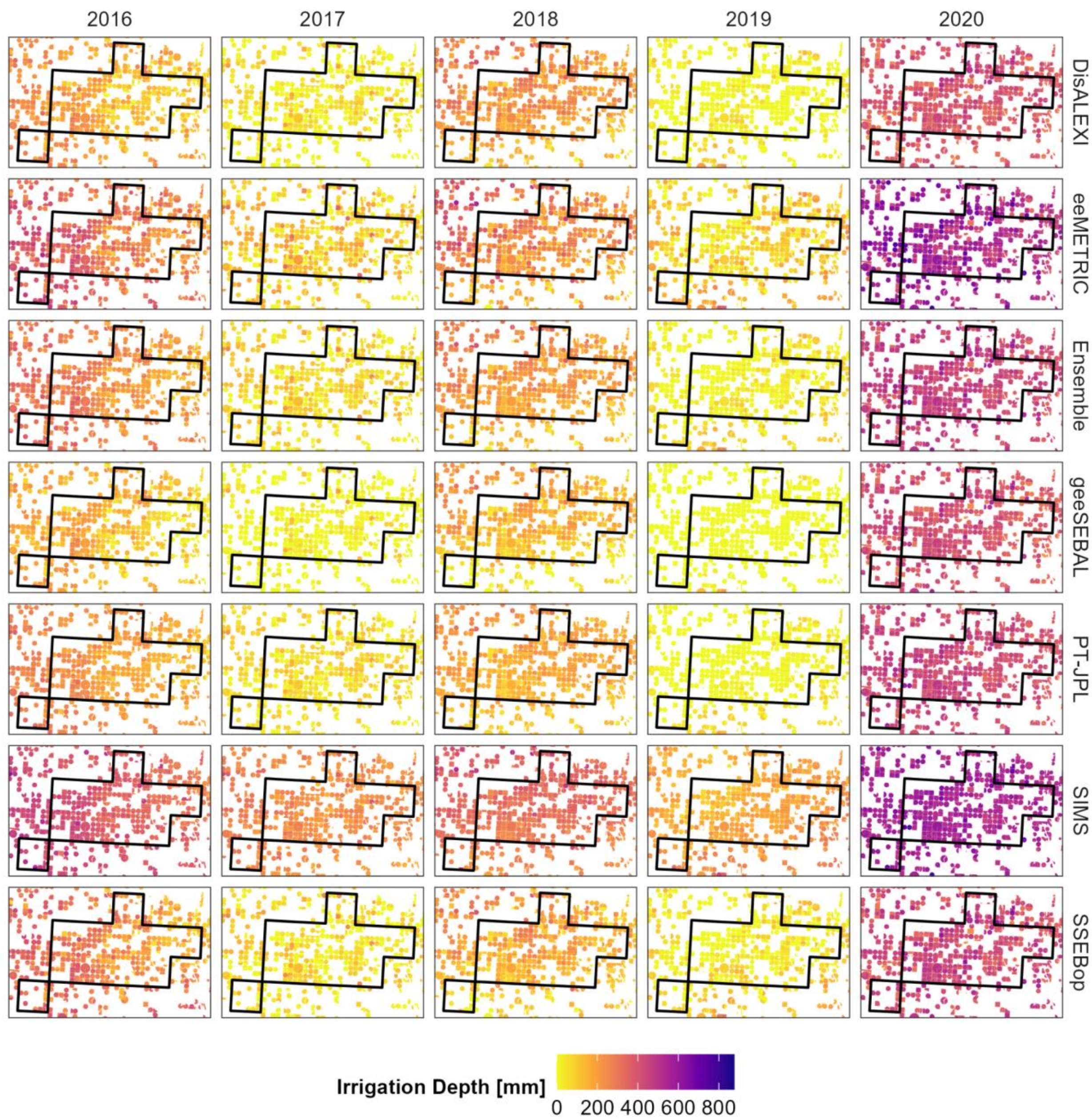

1068
1069 Figure S14. Same as Figure S6, but irrigation calculated using total growing season precipitation
1070 instead of effective precipitation.
1071

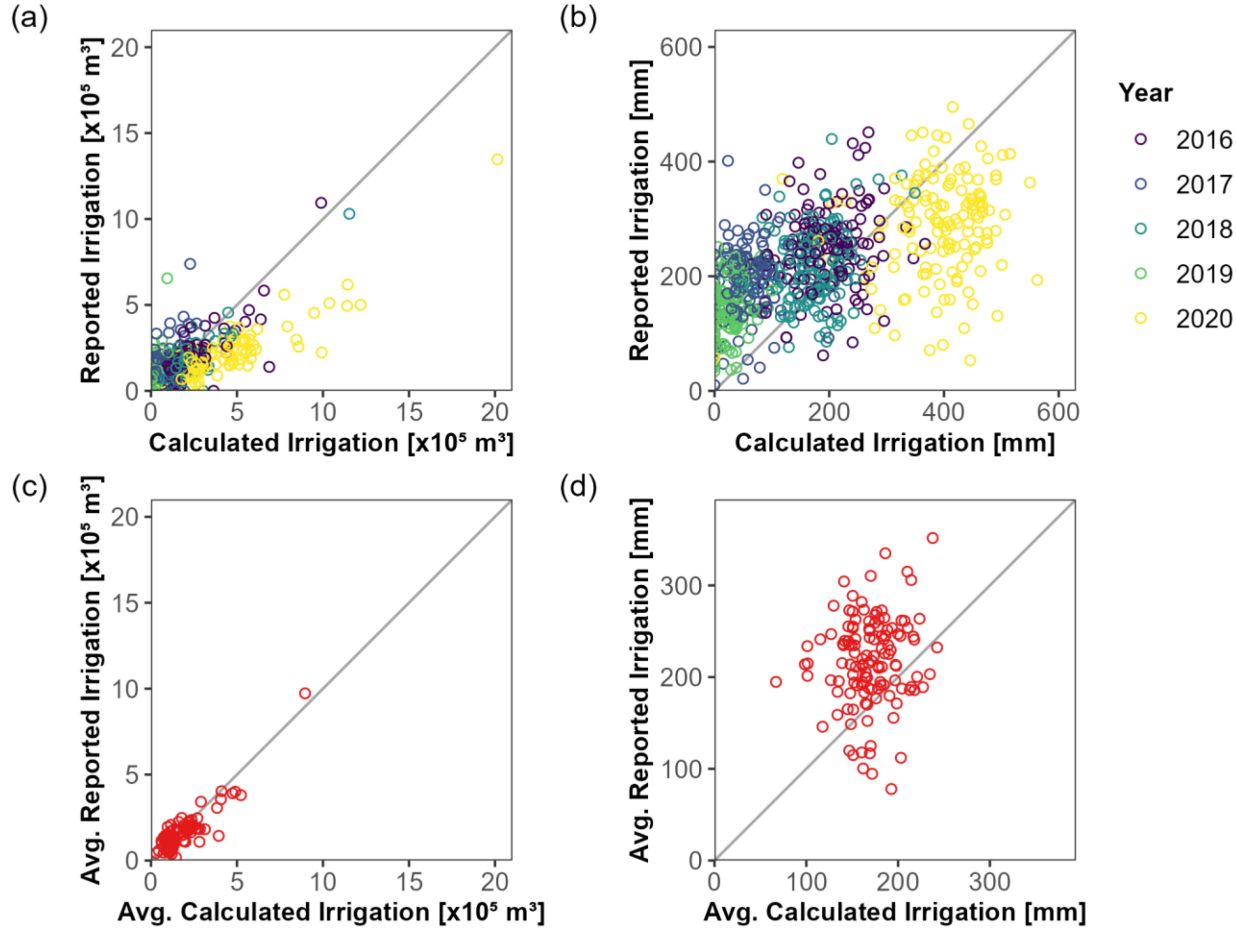

Figure S15. Same as Figure 5, but using precipitation in irrigation calculations instead of effective precipitation.

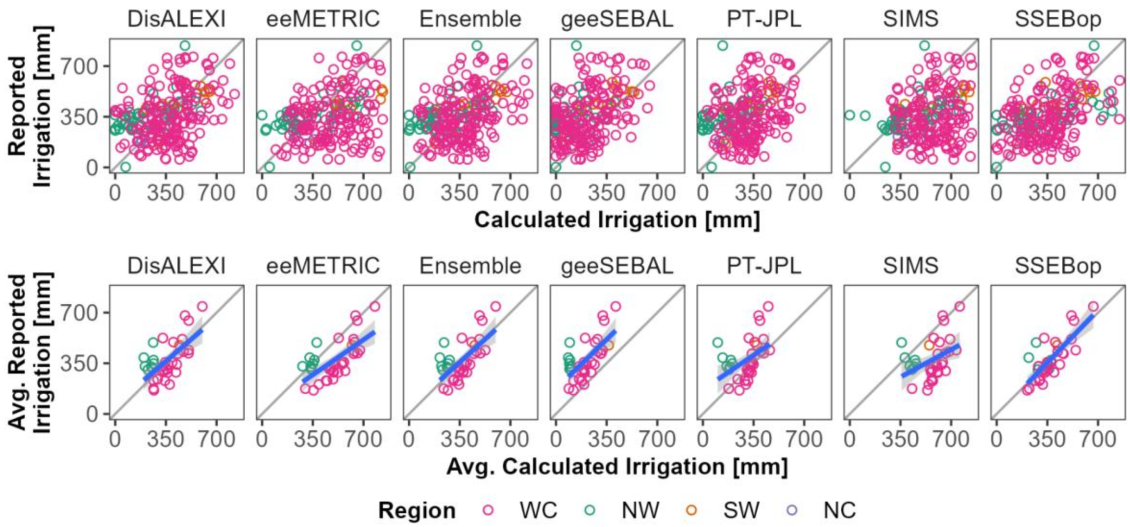

Figure S16. Same as Figure 7, but using precipitation in irrigation calculations instead of effective precipitation.

Table S2. Same as Table 2, but using precipitation in irrigation calculations instead of effective precipitation.

	MAE [mm]		**Bias [%]**		**Slope**		**R^2**	
Model	*Annual*	*Multi-Year*	*Annual*	*Multi-Year*	*Annual*	*Multi-Year*	*Annual*	*Multi-Year*
DisALEXI	159	87	-2.1	-3.7	0.36	0.86	0.15	0.40
eeMETRIC	209	140	36.2	33.6	0.28	0.69	0.15	0.45
Ensemble	154	85	0.1	-1.5	0.40	0.91	0.18	0.44
geeSEBAL	194	169	-44.3	-45.3	0.47	0.97	0.20	0.44
PT-JPL	160	99	-17.6	-19.2	0.37	0.68	0.11	0.21
SIMS	237	204	55.5	52.2	0.23	0.54	0.07	0.16
SSEBop	158	62	0.2	-1.3	0.39	1.04	0.21	0.61
Average	*181*	*121*	*4.0*	*2.1*	*0.36*	*0.81*	*0.15*	*0.39*

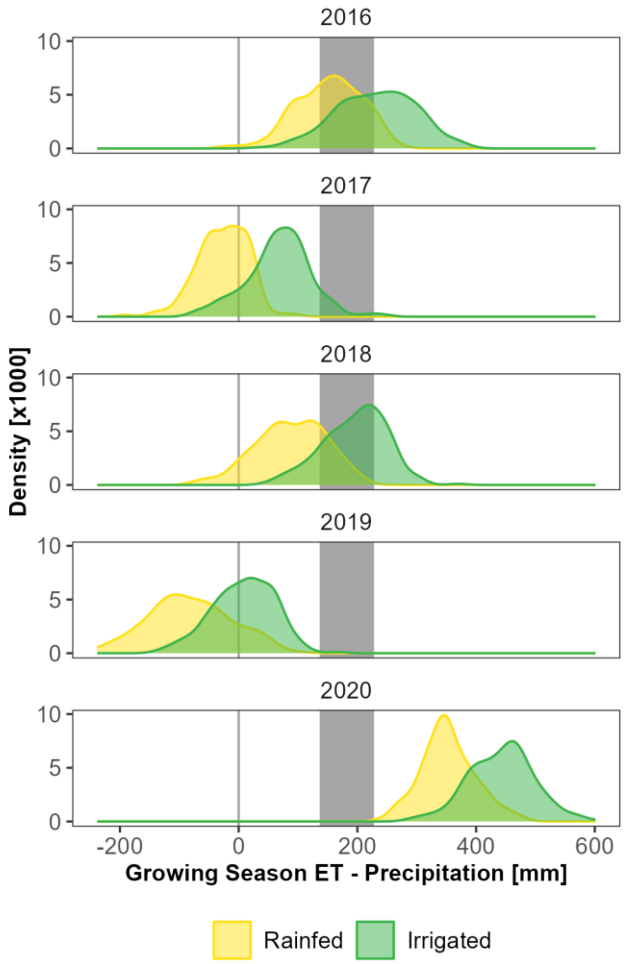

Figure S17. Same as Figure 8, but using precipitation instead of effective precipitation.

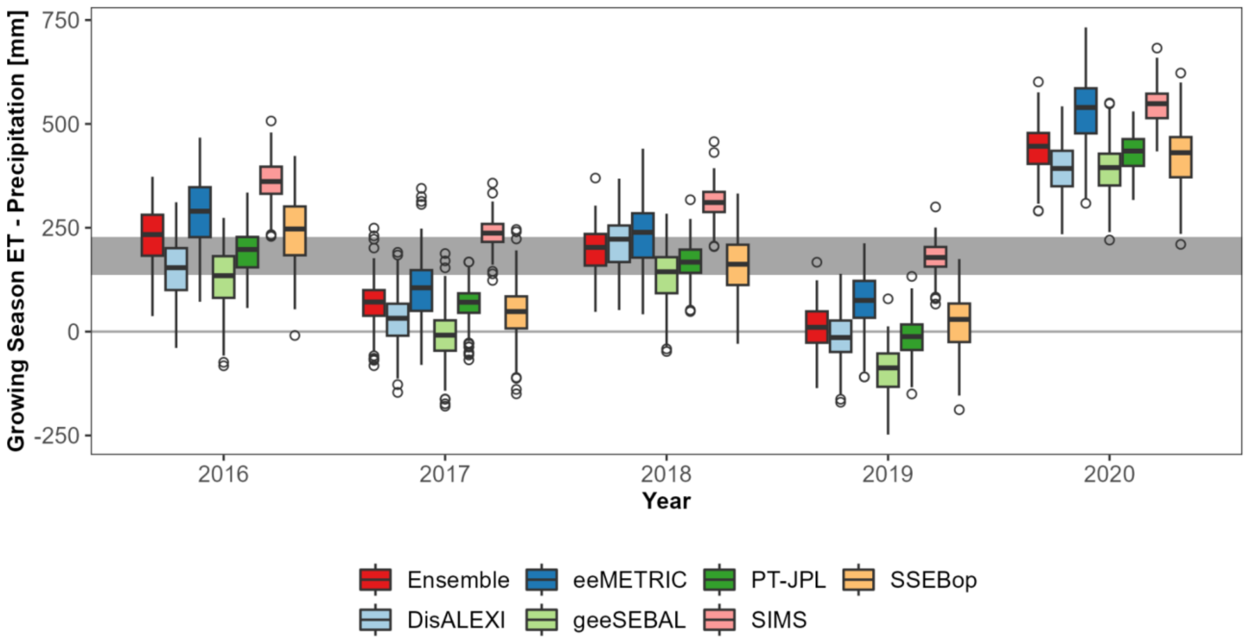

Figure S18. Same as Figure 9, but using precipitation instead of effective precipitation.

Section SI4. Comparison between radar and gridMET precipitation data.

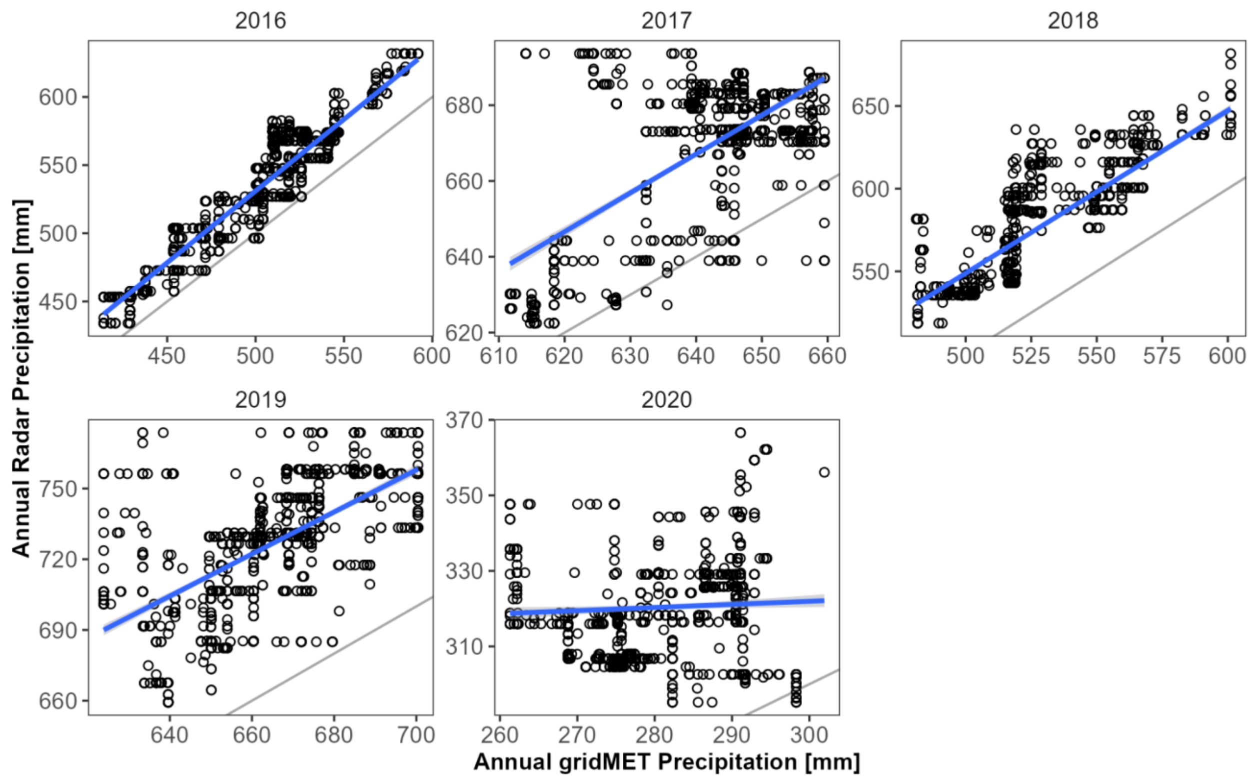

Figure S19. Comparison between gridMET- and National Weather Service Advanced Hydrologic Prediction Service radar precipitation data for all fields within the SD-6 LEMA. ET-based irrigation calculations use the growing season as the timescale of aggregation.

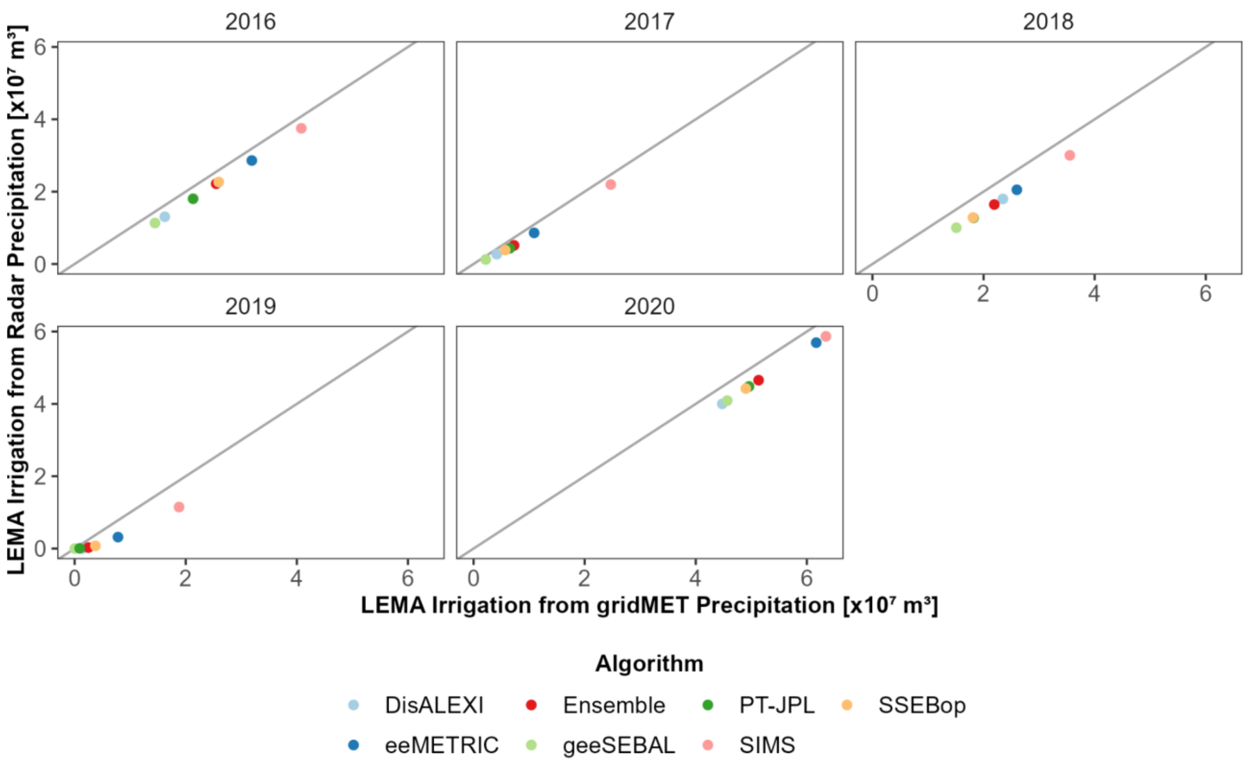

Figure S20. Comparison between LEMA total irrigation estimated using gridMET data and radar precipitation data for each model and year. ET-based irrigation calculations use the growing season as the timescale of aggregation. The 1-1 line is included in each plot.

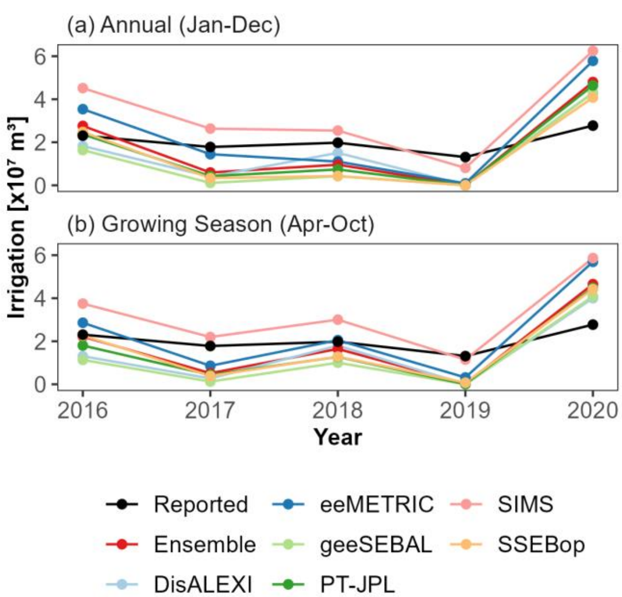

Figure S21. Comparison to reported irrigation volumes for estimated irrigation using OpenET data and radar precipitation for the entire SD-6 LEMA.

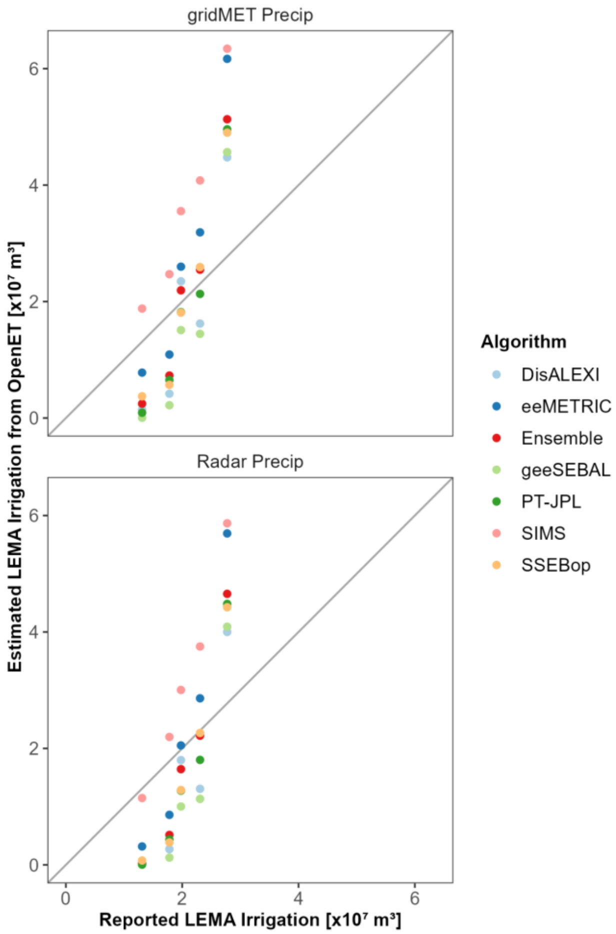

Figure S22. Comparison to reported irrigation volumes for estimated irrigation using OpenET data and (top) gridMET precipitation and (bottom) radar precipitation for the entire SD-6 LEMA. ET-based irrigation calculations use the growing season as the timescale of aggregation.

Section SI5. Additional figure related to WRG-scale WIMAS-OpenET comparison.

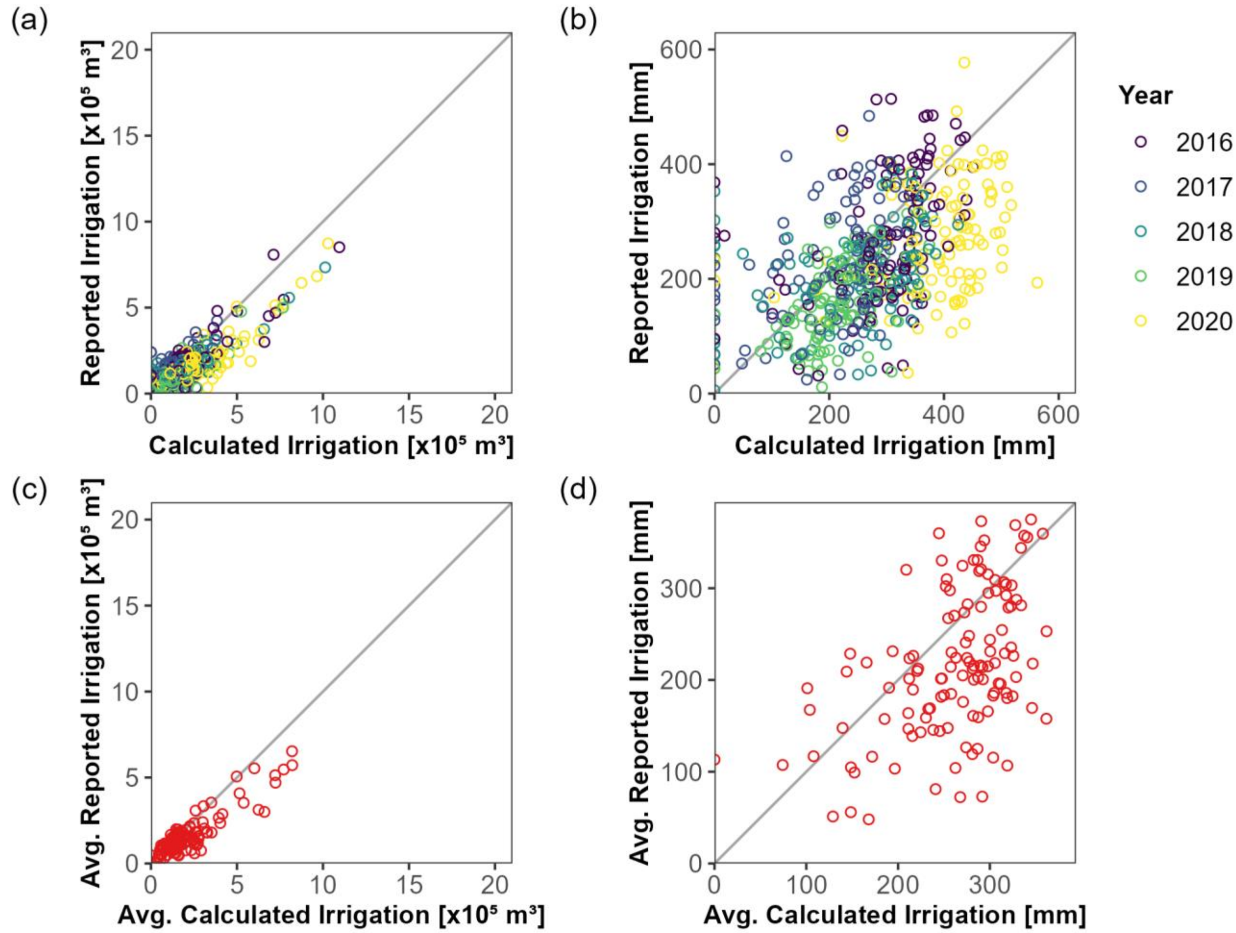

Figure S23. Same as Figure 5, but only for WRGs where reported and calculated irrigated area agreed within 10% (i.e., orange points in Figure 6). Since there were relatively few WRGs with good irrigated area agreement within the SD-6 LEMA, we also included WRGs with agreement within 10% from a buffer area surrounding the SD-6 LEMA. Each panel shows: (a) Annual irrigation volume for each WRG; (b) Annual irrigation depth for each WRG; (c) Average irrigation volume for each WRG; (d) Average irrigation depth for each WRG. In each plot, the gray line shows a 1:1 agreement between reported and calculated irrigation.

Section SI6. References in supplemental material

Deines, J. M., Kendall, A. D., Crowley, M. A., Rapp, J., Cardille, J. A., & Hyndman, D. W. (2019). Mapping three decades of annual irrigation across the US High Plains Aquifer using Landsat and Google Earth Engine. *Remote Sensing of Environment*, *233*, 111400. https://doi.org/10.1016/j.rse.2019.111400

Deines, J. M., Kendall, A. D., Butler, J. J., Basso, B., & Hyndman, D. W. (2021). Combining Remote Sensing and Crop Models to Assess the Sustainability of Stakeholder-Driven Groundwater Management in the US High Plains Aquifer. *Water Resources Research*, e2020WR027756. https://doi.org/10.1029/2020WR027756